# Diagenesis in limestone-dolostone successions after 1 million years of rapid sea-level fluctuations: A case study from Grand Cayman, British West Indies.

Min Ren, Brian Jones

*Department of Earth and Atmospheric Sciences, University of Alberta, Edmonton, Alberta, Canada T6G 2E3*

*E-mail address: mren@ualberta.ca*

**Abstract**

Meteoric diagenesis in young marine carbonate sediments has commonly been linked to fluctuations in Quaternary glacio-eustatic sea levels. The extent to which these sea-level changes are recorded in these carbonate successions, however, remains questionable. This is amply demonstrated by the diagenetic record found in the limestones and dolostones of the Cayman Formation (Miocene) on the Cayman Islands. On the eastern part of Grand Cayman, dolomitization that ceased by 1 million years ago created an architecture whereby the limestones in the central part of the island were surrounded by dolostones in coastal areas of the island. Since then, the upper 90 m of the Cayman Formation has been repeatedly cycled through many different marine and meteoric diagenetic zones as large, rapid eustatic oscillations in sea level affected the island. The records of these diagenetic cycles in the dolostones and limestones are, however, different and impossible to match to the cyclic changes in sea level. In the peripheral dolostones, post-dolomitization diagenetic features are sparse. In contrast, the limestones in the interior of the island exhibit a wider variety of meteoric diagenetic features, including extensive dissolution and calcite cementation. The dolostones have low porosity (< 10%) and permeability, whereas the limestones are characterized by high porosity (up to 50%), especially in the lower and middle parts of the studied limestone succession. The different phases of diagenesis found in the limestones, however, cannot be specifically matched to any sea level fluctuations that have affected these successions. This issue is further exemplified by the fact that that the last marine transgression over the last ~16,000 years ago appears to have left no tangible record. The analysis of this succession clearly demonstrates that not all diagenetic regimes will be recorded in the fabrics of limestones or dolostones.

**Keywords:** Diagenesis; sea level; Grand Cayman; Miocene; dolostone

## 1. Introduction

Before burial, most marine carbonate sequences have undergone significant shallow marine and meteoric diagenetic changes. In younger rocks like those found in Holocene successions (Land and Goreau, 1970; Ginsberg et al., 1971; Schroeder, 1972; James et al., 1976; Buchbinder and Friedman, 1980; Lighty, 1985; Budd and Land, 1990) and Pliocene–Pleistocene successions (Steinen and Matthews, 1973; Buchbinder and Friedman, 1980; Aïssaoui et al., 1986; Quinn and Matthews, 1990; Beach, 1995; Melim, 1996; Braithwaite and Camoin, 2011), diagenetic features have been linked to the rapid and high-amplitude changes in sea level that have been ongoing since the Pleistocene. Given that the positions of sea level, the water table, and the vadose zone are intimately linked (e.g., Longman, 1980; Quinn, 1991), the diagenetic fabrics in these rocks should reflect the changes caused by sea level fluctuations. Accordingly, many sequences of diagenetic fabrics have been linked to sea level oscillations (e.g., Aissaoui et al., 1986; Hardie et al., 1986; Quinn, 1991; Beach, 1995; Sherman et al., 1999) and models have been developed to show how diagenetic patterns develop in response to high-frequency glacio-eustatic sea-level cycles (Matthews and Frohlich, 1987; Whitaker et al., 1997). Such observations and models have been fundamental to the development of early diagenetic histories for carbonate successions of all ages. They are, however, predicated on the assumption the carbonate successions will contain a diagenetic record that fully reflects every diagenetic regime that it has experienced. But this is not always the case, as has been shown in studies from carbonate platforms such as Moruroa (Braithwaite and Camoin, 2011) and Bermuda (Vollbrecht and Meischner, 1996).

Isolated carbonates islands such as Grand Cayman, which are surrounded by deep oceanic waters, are highly sensitive to sea-level fluctuations. On the east end of Grand Cayman (Fig. 1), the carbonate bedrock is formed largely of the Miocene Cayman Formation (Fig. 2), which encompasses sediments that were deposited on an isolated bank (Jones and Hunter, 1989; Jones et al., 1994b). There, the central part of the island is formed largely of limestones whereas the bedrock in the coastal areas is formed entirely of dolostone (e.g., Jones et al., 1994b; Der, 2012). The fact that dolomitization took place prior to the onset of the rapid high amplitude glacio-eustatic changes in sea levels that started about 1 million years ago further complicates the diagenetic history of the succession. This situation also contrasts sharply with other areas in the world (e.g., Bermuda, Enewetak) where diagenesis triggered by eustatic changes in sea level acted on relatively young Holocene limestones that had not been previously dolomitized.

This study focuses on one cored well (GFN-2, 92.2 m deep) that was drilled in the limestone succession in the centre of the island, and two wells (RWP-2, 94.6 m deep; and ESS-1, 77.4 m deep) that penetrated the dolostone successions in the coastal areas (Fig. 1B, C). Over the last 1 Ma, sea-level has fluctuated from about -140 to +20 m relative to modern sea-level (Fig. 3), as has been shown in numerous studies (e.g., Siddall et al., 2003; Miller et al., 2005; Liseicki and Raymo, 2005; Naish and Wilson, 2009; Rohling et al., 2014). For the cored wells on the east end of Grand Cayman, this sea-level curve suggests that sea level was below or close to the base of GFN-2 on at least 11 occasions and close to or above the top of GFN-2 during 11 periods (Fig. 3). Such fluctuations also meant that the hydrological zones on the island were constantly moving up and down through the bedrock of the island. Thus, from a theoretical perspective, the diagenetic history of the limestones and dolostones in GFN-2, RWP-2, and ESS-1 should be complex and reflect the ever-changing diagenetic regimes that they have experienced. In particular, it might be expected that these rocks should contain a clear record of the progressive change in the hydrological zones caused by the transgression that has taken place over the last 20 kyr as sea-level has risen since the lowstand during the Last Glacial Maximum that was ~120 m below present day sea level (e.g., Peltier and Fairbanks, 2006; Clark et al., 2009). Accordingly, the rocks in the three cored wells on Grand Cayman were examined to determine if (1) the diagenetic fabrics reflect the numerous transgressive–regressive cycles (Fig. 3) that have affected these rocks over the last 1 million years, (2) the limestones and dolostones responded differently to these sea level oscillations, and (3) they provide any record of the rapid transgression that has passed through the rocks over the last 16,000 years. Although based on Grand Cayman, the results of this study have implications for carbonate successions of all ages because it questions the premise that carbonate rocks will always contain evidence of all the diagenetic zones in which they have been placed throughout their evolution.

## 2. Geological and hydrological settings

The Cayman Islands (Grand Cayman, Cayman Brac, and Little Cayman) are located on separate fault blocks that are part of the Cayman Ridge (Matley, 1926) (Fig. 1A). Grand Cayman, the largest island, has a low-lying interior that is generally < 3 m above sea level (asl) with a peripheral rim that rises up to 13.5 m asl around the eastern margin of the island (e.g., Jones et al., 1994a; Jones and Hunter, 1994b; Liang and Jones, 2014). The island has been tectonically stable over the last 500 kyr (Vézina et al., 1999) and probably over the past 5 Ma (Blanchon and Jones, 1995).

The surface to shallow subsurface carbonate succession on the Cayman Islands belongs to the Bluff Group that Jones et al. (1994a) divided into the Brac Formation (Oligocene), Cayman Formation (Miocene), and Pedro Castle Formation (Pliocene). The Bluff Group is unconformably overlain by the Pleistocene Ironshore Formation (Fig. 2). All of these formations are bounded by unconformities that formed during sea-level lowstands (Jones et al., 1994a).

The Cayman Formation crops out at the surface over most of the eastern part of Grand Cayman (Fig. 1B, C). In this area, the formation around the periphery of the islands is formed entirely of dolostones whereas the interior is formed largely of limestones that contain varying amounts of dolomite (Fig. 1C). This pattern is supported by the analysis of all available outcrops and samples from 43 wells that have been drilled over the last 15 years (e.g., Jones et al., 1994b; Der, 2012). For the purposes of this study, attention is focused on (1) well GFN-2 from the interior of the island because it is the only well in that area that was fully cored to a depth of 92.2 m, (2) well RWP-2, located on the northeast corner of the island, 4.5 km ENE of GFN-2 at 068.5°, that was cored to a depth of 94.6 m, and (3) well ESS-1, located 4.1 km south of GFN-2, that was drilled, partly cored, and sampled by well cuttings to a depth of 77.4 m (Fig. 1B). The successions in wells RWP-2, GFN-1, and ESS-1 clearly illustrate the lateral and vertical distribution of the dolostones and limestones (Fig. 1C) that are herein considered to be part of the Cayman Formation because there is no evidence of any stratigraphic boundary that would place them in different formations. Furthermore, there is no evidence of folding or faulting of the strata between these areas. On the basis of the stratigraphy and $^{87}Sr/^{86}Sr$ ratios, the dolomitization that probably took place during the late Miocene (Budd, 1997; Jones and Luth, 2003; Zhao and Jones, 2012), Pliocene (Pleydell et al., 1990), and possibly during the Pliocene to early Pleistocene (Budd, 1997; Jones and Luth, 2003; Zhao and Jones, 2012) was mediated by seawater. Critically, this means that the limestone core and peripheral dolostone scheme has been in place for at least the last 1 million years. Irrespective of the exact timing of the dolomitization, it is readily apparent that it took place before the onset of large, rapid sea-level oscillations that have taken place over the last 1 million years.

Three main unconfined freshwater lenses are housed in the Cayman Formation on Grand Cayman, namely the East End, North Side, and Lower Valley lenses (e.g., Mather, 1971; Ng et al., 1992). The irregular configurations of the lenses have been attributed to the attitude and orientation of the joint and fissure systems (Ng et al., 1992). Generally less than 20 m thick, these lens are capped by water tables that are generally < 0.5 m asl (Ng et al., 1992). A thick mixing zone (> 20 m) has developed between the freshwater and saline water zones in response to the tide-generated hydrodynamic dispersion (Ng and Jones, 1995).

## 3. Methods

This paper is based largely on the analysis of three wells (EES-1, GFN-2, RWP-2) drilled on the eastern part of Grand Cayman (Fig. 1B). They were selected from 43 wells that have been drilled in this area because they are the deepest wells in the areas of interest, and GFN-2 and RWP-2 were completely cored and EES-1 was partly cored with cuttings collected from the part that was not cored.

Well GFN-2 was cored to a depth of 92.2 m with an average core recovery rate of 63%. This well is located 6 m east of GFN-1, which was an exploratory well drilled to 121.9 m in 2011 but not cored. Wells RWP-2 and ESS-1 are located in the coastal areas of the island (Fig. 1B). Drilling of RWP-2 (in 1993) yielded continuous cores to a depth of 94.1 m below present sea level (bsl) with an average core recovery rate 97%. Well ESS-1, located 4.1 km south of GFN-2, was cored to 25 m bsl with average core recovery 88%, and sampled by well cuttings to a depth of 77.4 m (Fig. 1B). Sixteen groundwater samples from GFN-1 were collected from surface to the base of the wells for chemical analysis. Present-day hydrological zones are defined following the scheme of Ng et al. (1992). Thus, the freshwater zone, mixing zone, and saline zone are divided by 600 mg/L and 19,000 mg/L chloride contents, respectively. The distribution of the groundwater zones in well RWP-2 is based on 7 groundwater samples from well EEZ-1 (~2 km SSE of RWP-2 and ~350 m from the coast) that is the nearest well to RWP-2 from which water samples are available (Fig. 1B).

For GFN-2, whole core porosity and permeability ($K_{max}$, $K_{90}$, $K_{vert}$) were measured from 10 core pieces (5 cm in diameter, 13 to 22 cm long). For RWP-2, porosities were acquired from 59 core plugs. These analyses were performed by Core Laboratories Ltd., Calgary, Alberta, Canada.

The mineral compositions of whole-rock powders for 59 samples from GFN-2, 62 samples from RWP-2, and 49 samples from ESS-1 were analyzed by X-ray diffraction analysis (XRD) following the procedure of Jones et al. (2001). The results allow determination of the mol % of $CaCO_3$ in the dolomite (%Ca), and the percentages of calcite, high calcium dolomite (HCD, %Ca > 55%), and low calcium dolomite (LCD, %Ca < 55%) of the samples. The accuracies for these analyses are ±10% for the proportion of each population of dolomite and ±0.5% for the %Ca of each population (Jones et al., 2001).

Microscopic components and diagenetic features are based on the analysis of 59 thin sections from GFN-2 and 41 thin sections from RWP-2. All thin sections from GFN-2 were impregnated with blue epoxy in order to highlight the porosity, and stained with Alizarin Red S to allow discrimination of the calcite and dolomite. Thin sections from RWP-2 were stained with Alizarin Red S.

Carbon and oxygen stable isotope analyses were obtained for 35 samples from GFN-2 that contained various amount of calcite and dolomite. Isotope analyses for dolomite were obtained for 31 samples from RWP-2. These analyses were performed by Isotope Tracer Technologies Inc. (Waterloo, Canada) using a DELTA$^{Plus}$ XL Stable Isotope Ratio Mass Spectrometer (IRMS) that is coupled with a ConFlo III interface and EA1110 Elemental Analyzer. All results are reported against the Vienna Peedee Belemnite (VPDB). Standards were run before, during, and after analysis of the samples in order to maintain accuracy. The error margin for the $\delta^{18}O$ and $\delta^{13}C$ is ± 0.1‰.

## 4. Results

### *4.1. Well GFN-2*

#### *4.1.1. Sedimentary facies*

The Cayman Formation in well GFN-2 contains a diverse array of facies that are herein grouped into facies associations FA-I, FA-II, and FA-III (Fig. 4).

FA-I, in the lower part of the core (53 to 92.2 m), is formed mainly of skeletal rudstones and floatstones that contain domal (mainly *Leptoseris*) and branching (*Stylophora, Porites*) corals, green algae (mainly *Halimeda*), red algae, bivalves, gastropods, and benthic foraminifera (mostly *Amphistegina).* Mudstones with planktonic foraminifera occur at two intervals (63.0 to 68.7 m, and 80.0 to 88.0 m; Fig. 4). In general, both mudstone intervals transition upwards into coralline rudstones or floatstones through *Halimeda*-dominated facies or *Amphistegina*-dominated facies (Fig. 4).

FA-II, in the middle part of the succession (29 to 53 m), is formed largely of mudstone that contains planktonic foraminifera (mainly *Globigerinoides*?, *Globorotalia*?) and peloids formed by micritization of skeletal grains that are similar in size to the planktonic foraminifera.

FA-III, from the upper part of the formation (6 to 29 m) is formed largely of grainstones (Fig. 4). It is differentiated from the underlying FA-II by the presence of numerous benthic foraminifera (mainly *Amphistegina)*, numerous micritized grains, scattered bivalve fragments, and scattered coral fragments (mainly small-diameter *Stylophora).*

*4.1.2. Mineralogy*

Apart from the upper part of the succession (6 to ~9 m), which consists of calcareous dolostone (10% < %calcite < 50%), the Cayman Formation in GFN-2 is formed of limestone (< 10% dolomite) and dolomitic limestone (10–50% dolomite). On average, the rocks are 85–90% calcite, which includes the grains, matrix, and cements (Fig. 4). All of the dolomite is nonstoichiometric with 56.7 to 58.9%Ca and an average of 57.78%Ca.

*4.1.3. Porosity and permeability*

Porosity in GFN-2 (Fig. 4) ranges from 15.0 to 50.6% (mean = 43.9 ± 5.7%, n = 10), whereas permeability ($K_{max}$) ranges from 21.8 to 520.0 mD (mean = 306.13 ± 161.35 mD, n = 10). In nine out of the ten samples, $K_{max}$ is greater than $K_{vertical}$. Porosity and permeability ($K_{max}$) are positively correlated (Fig. 4). The lowest porosities (<20%) and permeabilities (<70 mD) are found in the upper part of the succession (6–14.5 m), whereas samples with higher porosity (>35%) and permeability (>130 mD) came from the middle and lower part of the succession (14.5–92.2 m).

*4.1.4. Diagenetic zones*

The Cayman Formation in GFN-2 is characterized by a wide array of diagenetic features, including micritization, dolomitization, five types of calcite cement, limpid dolomite, and dissolution. The succession is divided into diagenetic zones DZ-I, DZ-II, and DZ-III based on the types and distribution of these diagenetic fabrics (Fig. 4). There is no obvious correlation between the diagenetic zones and the facies associations.

DZ-I, from 92.2 m (base of well) to 35.5 m, is characterized by poorly cemented limestones with high porosities (Figs. 4, 5). The upper boundary is defined by the appearance of thin isopachous rims of microcrystalline calcite cement around the allochems (Fig. 4). Dissolution is common throughout this interval with almost complete leaching of aragonitic allochems such as the bivalves, gastropods, and corals (Fig. 5). Foraminifera were dissolved to varying degrees (Fig. 5E). Most red algae, however, are well preserved. Calcite cement is rare, being restricted to scattered dogtooth crystals in the basal part of the succession below 88 m (Fig. 5F, G). Limestones in this part of the succession have porosities of 36.1 to 50.6% and $K_{max}$ of 132 to 560 mD (Fig. 4).

DZ-II, from 14.5 to 35.5 m, is characterized by limestones that are partly cemented by microcrystalline calcite, have intermediate porosities, and extensive dissolution features (Fig. 4, 6). The upper boundary at 14.5 m marks the disappearance of microcrystalline calcite cement and a significant increase in the diversity of diagenetic features (Fig. 4). Microcrystalline calcite cement is ubiquitous throughout this interval. There is a notable increase in the thickness of the isopachous rims around the allochems from ~5 μm at the base to 30 μm at the top (Fig. 6). This is accompanied by a gradual increase in the amount of cement, from <15% at the base to ~50% at the top. Pervasive micritization, like that in DZ-I, and leaching of skeletal grains is ubiquitous in DZ-II. One sample from 24.1 m had a porosity of 36.8% and $K_{max}$ of 224 mD.

DZ-III, from 6.0 to 14.5 m, is formed of dolostones/dolomitic limestones that have low porosities (Fig. 4). It is separated from DZ-II by its higher diversity of diagenetic features and its lower porosity (15.0–19.7%) and permeability ($K_{max}$, 21.8–68.7 mD). Rocks in this section are characterized by the following:

- Numerous skeletal grains that are now represented only by micrite envelopes or were transformed into peloids by pervasive micritization (Fig. 7A).
- Dolomite is present as (a) limpid crystals, commonly ~ 50 μm long, on peloidal and skeletal substrates (Fig. 7B, C), and (b) crystals, 20–50 μm long, that fill pores (commonly

interparticle); some crystals are clear whereas others have dirty cores and clear rims (Fig. 7).

- Hollow dolomite crystals that are commonly filled with blocky calcite cement (Fig. 8A, B).
- Calcite cements that include (a) bladed crsytals in the lower part (DZ-III-1; 10.4–14.5 m), that formed isopachous rims 30 to 100 μm thick around grains and the chamber walls of skeletal grains (Fig. 8C), (b) drusy crystals, which typically overlies the bladed calcite, formed of crystals that increase in size from 5 to 50 μm towards the centre of the pores (Fig. 8C, D), and (c) blocky crystals, 50 to 300 μm long (Figs. 7, 8A, B), which was the last cement precipitated and commonly fills many of the cavities in the upper part of the interval (DZ-III-2; 6.5–10.4 m). Most pores in DZ-III are completely occluded by these three cements.

*4.1.5. Stable isotopes*

The $\delta^{18}O$ of the calcite ranges from -4.06 to +1.63‰ (mean = -0.87 ± 1.45‰, n = 35), and the $\delta^{13}C$ ranges from -7.63 to +2.10‰ (mean = -1.08 ± 2.57‰, n = 35). Overall, the $\delta^{18}O$ and $\delta^{13}C$ of the calcite are highly correlated ($\delta^{13}C \approx 1.6\ \delta^{18}O + 0.31$, $R^2 = 0.82$) (Fig. 4). Both isotopic values vary between the diagenetic zones: (1) the average $\delta^{18}O$ increases from -2.73‰ (DZ-I) to -2.02‰ (DZ-II) and +0.13‰ (DZ-III), and (2) the average $\delta^{13}O$ values from -6.23‰ (DZ-I) to -2.57‰ (DZ-II), and +0.77‰ (DZ-III).

Dolostones from upper part of the succession (6.5-27.6 m) have $\delta^{18}O$ from -0.08 to +2.16‰ (+0.64 ± 0.66‰, n = 9), and $\delta^{13}C$ from -1.63 to +1.59‰ (-0.25 ± 0.91‰, n = 9) (Fig. 4).

*4.2. Wells RWP-2 and ESS-1*

The depositional and diagenetic features in the Cayman Formation in well RWP-2 (Fig. 9) are based on Willson (1998) and analyses done in this study. The succession in well ESS-1 is essentially the same as that in RWP-2 (Fig. 10). Most of the following description is, however, based on the succession in well RWP-2 because it was completely cored to a depth of 94.6 m with a 98% recovery rate.

*4.2.1. Sedimentary facies*

The Cayman Formation in well RWP-2 is characterized by the coral-rhodolith floatstone–rudstone facies association (FA-IV) that includes the (1) *Stylophora* floatstone facies, (2) rhodolith branching coral floatstone facies, (3) rhodolith coral fragment rudstone–grainstone facies, (4) *Porites-Leptoseris-Montastrea-Stylophora* floatstone facies, and (5) *Leptoseris-Montastrea* floatstone facies (Fig. 9). There is no systematic pattern to the vertical stacking of these facies (Fig. 9). Cores from the upper 25 m of well ESS-1 reveals similar lithologies that dominated by skeletal grains derived from *Porites, Stylophora, Montastrea*, and rhodololiths (Fig. 10).

*4.2.2. Mineralogy*

The Cayman Formation in well RWP-2 is formed entirely of dolostone (Fig. 9). The same is true for well ESS-1 (Fig. 10) apart from minor amounts of calcite (<35%) in the upper 14 m of the well. Most of the dolostones (58 of 63 samples from RWP-2, and 43/50 of ESS-1) contain more LCD (average %LCD = 72.3% from RWP-2, and 83.6% from ESS-1) than HCD. HCD-dominated dolostones are restricted to the bottom part of RWP-2 (84–90 m), and the upper part of ESS-1 (10–20 m). All dolomite is nonstoichiometric with 54.4%Ca (RWP-2) and 53.2%Ca (ESS-1).

*4.2.3. Porosity*

Fossil moldic, interparticle, and fracture porosities dominate in RWP-2 and ESS-1. Porosity in the dolostones from well RWP-2 ranges from 1.7 to 29.2% with an average of 8.0 ± 5.4% (n = 50) (Fig. 9). Apart from two samples that have porosities of 29.2% (19 m) and 22.9% (21 m), the porosities are less than 10% (Fig. 9).

*4.2.4. Diagenetic zones*

The Cayman Formation in well RWP-2 is formed of finely crystalline dolostones that are characterized by low porosity, a complex array of limpid dolomite cements, and various types of cavity-filling sediments. This includes caymanite, which is a multicolored (white, red, blac), cavity-filling sediment (mudstone to grainstone) with laminae that dip at angles up to 60° (Jones, 1992).

The original limestones in the succession in RWP-2 were completely replaced by fabric-retentive dolostones that are composed of anhedral to subhedral crystals < 50 µm long. Three generations of cement are present:

- Generation 1 (G1), common throughout the succession, is formed of subhedral to euhedral dolomite crystals, 30–100 µm (average ~50 µm) long, that form isopachous rims around the cavities and between the allochems. These crystals are divided into unzoned (G1a), zoned with 2–5 layers of clear dolomite (G1b, Fig. 11D), and dolomite with a limpid dolomite core encased by a thin dark-colored, inclusion-rich zone (Jones 1984), that is then overlain by a zone of clear dolomite (G1c, Fig. 11B, F). The latter two zones are, in some examples, repeated.
- Generation 2 (G2), which commonly overlies G1, is formed of subhedral drusy to blocky crystals, 100–120 um long (Fig. 11E).

- Generation 3 (G3), found in only one sample at a depth of 3.5 m, is formed of calcite cement that overlies the dolomite cement.

Internal sediments that filled many of the cavities in the Cayman Formation in RWP-2 (Fig. 11A, C, F) include caymanite, skeletal wacke/pack/grainstones, and terra rossa. These cavity-filling sediments are characterized by various sedimentary structures such as graded laminae in the caymanite and typically have low porosity. The complex relationships between the cavity-filling sediments and cements include (1) sediments that filled cavities with no cement, (2) sediments that filled cavities that were lined with dolomite cements (mostly G1, Fig. 11A, C), and (3) dolomite cements (G1) that postdated the cavity fills (Fig. 11F).

Dolostones in the Cayman Formation in well RWP-2 are divided into diagenetic zones DZ-IV to DZ-VI (Fig. 9).

DZ-IV (45.8–94.6 m) is characterized by dolostones with low porosity (average 5.2 ± 2.8%) with G1 cements throughout. The upper boundary at 45.8 m, is defined by a significant increase in the amount of cavity-filling sediments. Dolostones in this part of the succession contain 5–17% dolomite cements (types G1b and G1c). The cavity-filling sediments are formed largely of caymanite with lesser amounts of skeletal wacke/pack/grainstones above 55 m and minor terra rossa at 52.8 m.

DZ-V (27.0–45.8 m), is characterized by dolostones with cavities of various sizes that have been filled with internal sediments (Fig. 9). The boundary between DZ-V and DZ-VI, placed at 27 m, marks a significant decrease in the cavity fills. The internal sediments are formed mostly of skeletal wacke/pack/grainstones. In some cavities, two or more types of internal sediment are stacked on top of each other; for example, caymanite on top of peloidal packstone (Fig. 11C).

Dolomite cements (type G1c) form < 3% of the rock. The average porosity (7.6 ± 5.2%) is higher than that in DZ-IV.

DZ-VI (0–27.0 m) consists of dolostones that are cemented primarily by type G1a cement, which forms ~6% of the rock. Calcite cement (G3) was found only in the uppermost sample at 3.5 m. Small amounts of terra rossa (0.5–1%) are present in the cavities at the top (3.5 m) and bottom (24.4 m). Porosities in this zone range from 2.4 to 29.2%.

*4.2.5. Stable isotopes*

The $\delta^{18}O$ value from 31 dolomite samples from well RWP-2 range from 2.38 to 4.21‰ (average 3.59 ± 0.36‰), and the $\delta^{13}C$ from 2.15 to 3.83‰ (average 3.26 ± 0.37‰) (Figs. 9, 12). There is no correlation between (1) the oxygen and carbon isotopes, and (2) the isotopic values and the %Ca.

## 5. Interpretation

### *5.1. Depositional environment*

There are significant differences in the sedimentary facies in the Cayman Formation found on the island periphery and interior as illustrated by comparing wells RWP-2 and ESS-1 with well GFN-2. Comparison of GFN-2 and RWP-2, for example, highlights the abundance of corals and rhodoliths in RWP-2 (Fig. 9) as opposed to the dominance of skeletal grains and rare corals in GFN-2 (Fig. 4). Given that there is no evidence of folding or faulting of the strata between these two localities, these contrasts must reflect original facies.

Numerous corals and photosynthetic algae in RWP-2 and ESS-1 indicate that the depositional environments around the edge of the island were characterized by normal marine conditions with open circulation between the bank edge and open ocean, probably within the photic zone. Corals from these areas are characterized by their variable morphologies (branching, domal, platy) that can be linked to a depositional spectrum that varied from high energy and low sedimentation settings to low energy and high sedimentation settings, as suggested by Willson (1998). The numerous rhodoliths found in these areas probably originated under relatively high-energy conditions. The recurring coral- and rhodolith-dominated facies found on the peripheral parts of the island (wells RWP-2 and ESS-1), indicate deposition on a bank edge to inner bank setting (Willson, 1998). This is consistent with the conclusion of Jones and Hunter (1994a).

In well GFN-2, FA-I, FA-II, and FA-III record progressive changes in the depositional conditions in the island interior through time. FA-I, in the lower part of the well, includes the *Leptoseris-Stylophora-Porites* floatstone/rudstone facies that is similar to the *Stylophora-Porites* and *Stylophora* associations described by Hunter (1994), and the branching coral-*Amphistigina* facies of Der (2012). Dominated by fragile branching corals, this facies represents coral thickets that grew on a sandy seafloor under moderate to low energy conditions with high sedimentation rates in water 10 to 30 m deep (Hunter, 1994; Der, 2012). The *Halimeda*-dominated facies and mudstone facies found in parts of FA-I probably formed under lower energy conditions.

FA-II (29-53 m), formed largely of mudstones with planktonic foraminifera, records deposition in a quite-water setting. *Globigerinoides,* the dominant species, is a shallow-water planktonic foraminifera that has inhabited the euphotic zone in waters 10–50 m deep since the Oligocene (Gupta, 2003). As such, FA-II probably developed while low energy conditions prevailed, possibly in deeper water than that associated with FA-I.

FA-III (6 to 29 m), with its *Amphistigina* and bivalve dominated wackestone to grainstone facies, has been found in other wells on the eastern part of Grand Cayman (Der, 2012). These facies probably developed under low- to high-energy conditions in water that was 10 to 20 m deep.

### 5.2. Diagenesis

Dolostones and limestones in the Cayman Formation have undergone extensive diagenetic modifications since the original sediments were deposited during the early to middle Miocene, with one of the main results being significant differences in the extent of dolomitization in different parts of the island. This is clearly evident on the eastern part of Grand Cayman where the Cayman Formation in GFN-2 consists largely of limestone (generally < 15% dolomite), whereas the successions in RWP-2 and ESS-1 are formed entirely of dolostone (Figs. 4, 9). For the purposes of this paper, the diagenetic history is considered relative to the pervasive dolomitization that affected the Cayman Formation. Based on stratigraphic relationships and the $^{87}Sr/^{86}Sr$ ratios, pervasive dolomitization on Grand Cayman has been attributed to either one phase, 2–5 Ma (Pleydell et al., 1990) or two phases, 6–8 Ma and 1.9–2.2 Ma (Jones and Luth, 2003). For Cayman Brac, two phases of dolomitization from 6–8 Ma and 1–5 Ma were proposed by Zhao and Jones (2012). Irrespective of the details, all of these studies argued that pervasive dolomitization had finished before 1 Ma. Critically, this means that the basic architecture of a peripheral dolostone and central limestone core for the Cayman Formation has been in place for at least 1 million years. Accordingly, the diagenetic history of the Cayman Formation on the eastern part of Grand Cayman can be divided into the pre- and post-dolomitization phases.

#### 5.2.1. Pre-dolomitization diagenesis and dolomitization

In GFN-2, pre-dolomitization diagenesis included extensive micritization of various allochems that took place on sea floor shortly after sediment deposition. This led to the formation of micrite envelopes around many allochems and the transformation of others to peloids. Textural evidence indicates that micritization took place before the onset of allochem dissolution.

Later processes, evident in well RWP-2, included (1) the development of fossil-moldic porosity as the aragonitic skeletons (e.g., corals) were dissolved, (2) the filling of cavities by internal sediments and cements, and (3) lithification. Cavity-filling sediments in RWP-2 include caymanite and skeletal wacke/pack/grainstones, which have been attributed to various marine and terrestrial processes (Jones, 1992). The fact that these cavity-filling sediments are pervasively dolomitized and have similar stable and radiogenic isotope signatures to the surrounding dolostone bedrock indicates that they were emplaced before dolomitization took place (Pleydell et al., 1990; Jones, 1992). These cavity-filling sediments and cements, which led to a significant reduction in porosity in RWP-2, are absent from the succession in GFN-2.

By the time pervasive dolomitization had ceased, there was a significant difference between the Cayman Formation found in the interior and the peripheral parts of the island. The peripheral succession was pervasively dolomitized, contained cavities that were largely filled by internal sediments and cements, and had low porosity. In contrast, the Cayman Formation in the interior of the island was formed largely of limestone, lacked cavity filling sediments and cements, and was highly porous. This stark contrast set the stage for post-dolomitization diagenesis.

*5.2.2. Post-dolomitization diagenesis*

Post-dolomitization diagenesis in well GFN-2, included dissolution and precipitation of calcite cements. In the upper part of the well (DZ-III, 6.5–14.5 m), the negative stable isotope values ($\delta^{18}O_{cal}$ = -2.73 ± 1.12‰, $\delta^{13}C_{cal}$ = -6.23 ± 0.95‰; Fig 12) and pervasive calcite cementation point to diagenesis in the meteoric-phreatic zone. Reduction in the proportion of the heavier isotopes in the calcite relative to the original sediments points to alteration by isotopically light freshwater (Fig. 12). Occlusion of pores by drusy, blocky, and isopachous calcite cements implies precipitation in the phreatic zone where pores were filled by freshwater. The absence of vadose cements in this interval may reflect (1) vadose waters that were unsaturated with respect to calcite/aragonite and/or physical-chemical conditions in the pores and cavities that were unfavorable for precipitation, (2) water that flowed through the vadose zone in GFN-2 area so rapidly that precipitation did not take place, (3) vadose waters that did not flow through the rocks in the area where GFN-2 was drilled (cf., Thorstenson et al., 1972; Braithwaite and Camoin, 2011), and/or (4) removal by erosion of the rocks that originally contained evidence of vadose diagenesis.

In the middle part of GFN-2 (DZ-II and upper DZ-I, 14.5–60 m), carbon and oxygen isotopes gradually shift to positive values towards the base of the interval ($\delta^{18}O_{cal}$ from -3.18‰ to +0.99‰, $\delta^{13}C_{cal}$ from -4.45‰ to +1.85‰) (Figs. 4, 12). This may reflect either (1) diagenesis in a mixing zone where varying mixtures of freshwater and saline water produced gradual changes in the isotopic compositions of pore fluid with depth, or (2) an artifact of sampling with the analyzed samples including both the cements that were precipitated from isotopically lighter freshwater and the skeletal grains and matrix that formed from isotopically heavier marine waters. If the second possibility is applicable, then the whole-rock isotope values would be negatively correlated with the amount of cement in the samples. This is not true for the lower part of this interval (36.5–60.0 m) where both isotopes increase with depth even though calcite cement in this interval is absent. Thus, this middle interval of GFN-2, 45.5 m thick, probably represents a paleo-mixing zone.

Positive isotope values ($\delta^{18}O_{cal}$ = +0.57 ± 0.53‰, $\delta^{13}C_{cal}$ = +1.35 ± 0.49‰), and extensive dissolution of skeletal grains characterizes the lower part of the succession (lower DZ-I, 60–92.2 m) (Figs. 3, Fig. 10). This may indicate that the diagenetic fabric and isotopes in this interval resulted from modification by meteoric and saline phreatic diagenesis. According to the sea level curve for the last 1 myr (Fig. 3), sea level has dropped below the base of GFN-2 at least five. During those periods, the succession would have been subaerially exposed and pervasive dissolution of skeletal grains may have been mediated by meteoric diagenesis, particularly in the vadose zone. Positive carbon and oxygen isotopes of the limestone suggest saline water modification of the sediments when they were submerged in the saline water zone after meteoric dissolution had taken place. The basal part of this interval, below ~90 m, includes some dogtooth calcite cement that may be related to submarine diagenesis, as has been suggested for similar cements found on Grand Bahamas Bank (Melim et al., 1995) and Moruroa (Braithwaite and Camoin, 2011).

## 6. Discussion

The Miocene strata of the Cayman Formation in the interior and coastal parts of Grand Cayman contrast sharply in terms of their facies, mineralogy, porosity, permeability, diagenetic fabrics, and geochemical signatures. Spatial variability in diagenesis like this is evident in many carbonate platforms worldwide. Submarine cements are, for example, largely restricted to marginal facies and the degree of marine cementation commonly decreases from the peripheral to the central parts of a platform (James et al., 1976; Lighty, 1985; Aïssaoui et al., 1986; Marshall, 1986; Vollbrecht, 1990). On the eastern part of Grand Cayman, pervasive dolomitization was restricted to coastal areas where the large volumes of seawater needed for such diagenesis could be pumped through the rocks (cf., James et al., 1976; Marshall, 1986).

Early diagenesis, including cavity formation, filling of cavities with internal sediments and dolomitization, significantly reduced the porosity and permeability in the strata in these coastal regions. Although seawater still percolated through those dolostones during post-dolomitization times, the reduced porosity and permeability resulting from the earlier diagenesis caused decreased flow rates and curtailed diagenetic activity. Dolomitization of the coastal strata before 1 Ma was critical to the subsequent evolution of the strata on Grand Cayman because it (1) produces dolstones that were more less susceptible to the meteoric diagenesis that has taken place over the last 1 myr, and (2) it reduced porosity and hence impeded the flow of waters through the rocks.

The sea-level curve for the last 1 myr shows 16 highstand-lowstand cycles of various magnitudes that are characterized by rapid transgressions, short-lived highstands, and slow regressions (Fig. 3). Collectively, this means that the rocks in the basal parts (at ~ 94 m bsl) of wells RWP-2, GFN-2, and ESS-1 on Grand Cayman have experienced longer cumulative times of exposure than the rocks higher in the succession (Fig. 13). There is an almost linear relationship between the cumulative length of exposure time over the last 1 myr and the depth below present day sea level. For example, relative to present day sea level, strata in the Cayman Formation in wells RWP-2, GFN-2, and ESS-1 at 0 m, minus 50 m, and minus 94 m have, over the last 1 myr, been exposed for cumulative periods of ~ 950,000 years, 520,000 years, and 90,000 years, respectively (Fig. 13). Thus, it might be reasonable to expect that there should be some trends in the type and/or degree of diagenetic change that could be matched with the linear trend between depth and cumulative exposure time (Fig. 13). There are, however, no obvious correlations between any aspect of the diagenesis with either the repeated highstand-lowstand cycles or cumulative exposure time. In the upper part of GFN-2 (6.5–14.5 m), the sequence of calcite cements is simple with the limestones containing no more than two types of cement. Although those pores with two types of calcite cement may have evolved during different highstands, it is impossible to date those cements and they cannot, therefore, be linked to specific sea level highstands. Nevertheless, precipitation of these cements would have reduced the porosity/permeability and possibly affect fluid circulation during later times (cf., Braithwaite and Camoin, 2011). Similarly, there is no pattern to the distribution of the dissolution features. In GFN-2, for example, the degree of dissolution is consistent throughout the entire succession. This, however, may simply be the reflection of two factors. First, there was a relatively even distribution of the solubility-prone components throughout the succession. Second, all of these components may have been dissolved when they were first exposed to meteoric diagenesis during the first regressive cycle. This is plausible, especially if exposure to the atmosphere occurred during a time when there was a humid paleoclimate with high rainfall that allowed large volumes of freshwater to be flushed through the strata (cf., Li and Jones, 2013; Whitaker et al., 2006). Once the solubility-prone components were dissolved no further dissolution would take place even if the diagenetic conditions were suitable for such diagenesis. In the shallow part of the succession, diagenetic alteration dominated, with the surface zone being case hardened by pervasive calcite cement. This offers a stark contrast to the poorly cemented limestones in the deep part of the succession. Similar diagenetic patterns have been found in Mururoa (Aïssaoui et al., 1986), the Bahamas (Beach, 1995; Melim, 1996), Florida (Melim, 1996), and on Enewetak Atoll (Quinn, 1991).

The contrast in the amount of calcite cement between the coast and interior of Grand Cayman can probably be attributed to contrasts in the hydrological regimes associated with the establishment of freshwater lenses during sea-level highstands over the past 1 myr. Today, the

East End water lens on Grand Cayman is centrally located (e.g., Mather, 1971; Ng et al., 1992) and does not extend into the dolostones of the coastal areas (Fig. 1B). Meteoric calcite cement in the Cayman Formation in the interior part of the island is (1) stratigraphically controlled and restricted to particular depth intervals, (2) found in thin, dense, more or less stratiform horizons, and (3) increases towards the center of the island. This pattern is similar to that on Mururoa Atoll (Aïssaoui et al., 1986). On Grand Cayman, these cementation patterns probably developed in response to the positions of the hydrological zones that fluctuated in concert with the changes in sea level (cf., Whitaker et al., 1997; Melim et al., 2002) over the last 1 myr.

It seems probable that freshwater lens did develop during lowstands when sea levels were ~90 m bsl. This is supported by many modern examples of freshwater lenses that have developed beneath thick vadose zones on small islands like Grand Cayman, Cayman Brac (~40 m thick vadose zone; Mather, 1971; Ng et al., 1992) and Niue (30-70 m thick vadose zone; Jacobson and Hill, 1980; Wheeler and Aharon, 1997). It has also been shown that during the last sea level lowstand, when the water table was 120 m bsl, bank-wide phreatic lenses developed across the Grand Bahamas Bank and Cat Island (Beach, 1995). Determining the exact extent of the freshwater lens on Grand Cayman during those lowstands is difficult because the size and distribution of the lens is controlled by many factors, including topography, climate, geological structure, and platform size (e.g., Cant and Weech, 1986; Budd and Vacher, 1991; Beach, 1995; Vollbrecht and Meischner, 1996; Vacher, 1997). Irrespective, as sea level rose and fell during the transgressive-regressive cycles, the freshwater lens and its associated hydrological zones would have moved vertically through the strata in the upper part of the Cayman Formation. With such a scenario, it might be expected that these strata would contain substantial amounts of calcite cement and that the porosity would have been largely occluded. Most of the transgressive-regressive cycles over the last 1 myr were of short duration (Fig. 3) and it therefore seems probable that the situation was so dynamic that the hydrological zones were never established long enough to allow pervasive calcite cementation (cf., Steinen, 1974; Quinn, 1991). Alternatively, even if the freshwater lens were established, the water may have been chemically inactive and calcite precipitation impossible (cf., Melim, 1996; Melim et al., 2002).

Analysis of the diagenetic features in the Cayman Formation in wells GFN-2 has shown that there is no clear correlation between the different diagenetic features and the different diagenetic environments that the rock may have experienced over the last 1 myr. It is possible, however, that this simply reflects issues associated with the evolution of these rocks over an extended period of time. This notion, however, can be tested by considering the diagenesis that has taken place in the upper part of the Cayman Formation since the last transgression that started ~20 kyr ago (Fig. 14) when sea-level was 120 m bsl. During this progressive rise in sea-level rise, the Cayman Formation must have been subject to ever-changing hydrological regimes. Despite this, none of the diagenetic features in the Cayman Formation can be directly linked to any of the groundwater zones or hydrological conditions that existed during this transgressive phase (Fig. 14). Thus, it is readily apparent that this last dramatic transgression has left little or no record on the limestones and dolostones of the Cayman Formation on Grand Cayman.

## 7. Conclusions

The sediments that now form the Cayman Formation (Miocene) on Grand Cayman accumulated on a carbonate bank. Before the high-frequency, high-amplitude glacio-eustatic changes in sea levels that started ~1 Ma, the peripheral part of the island had been subject to marine diagenesis and dolomitization. Since then, oscillations in sea level have repeatedly placed the limestones and dolostones of the Cayman Formation into contrasting marine and meteoric diagenetic environments. The main conclusions reached in this study are:

- On the east end of Grand Cayman, partial dolomitization of the Cayman Formation, more than 1 million years ago, meant that limestones in the central part of the island were encircled by dolostones in coastal areas.
- Over the last 1 myr, limestones found in the interior of the island have undergone more diagenetic changes than the dolostones found in the coastal regions.
- Dissolution features and high secondary porosities evident in middle to lower parts of the limestone succession reflect diagenetic activity in vadose and/or phreatic zones that took place during sea-level lowstands.
- Pervasive meteoric cements are restricted to upper part of the limestone succession even though the entire succession has been repeatedly placed in the meteoric phreatic zone as sea level has oscillated.
- Dissolution features, which are relatively consistent throughout the limestone succession –n the interior of the island cannot be correlated with the cumulative exposure time over the last 1 myr and cannot be specifically matched to any of the numerous transgressive-regressive cycles that have affected the succession.
- The different generations of calcite cement, evident in some parts of the succession, cannot be matched with the multiple cycles of sea level fluctuations that have passed through the succession.
- The Cayman Formation does not seem to include any diagenetic fabrics that can be attributed to the last transgression that has affect the upper succession over the last 16,000 years.

The diagenetic fabrics evident in the limestones and dolostones of the Cayman Formation do not reflect the ever-fluctuating positions of the diagenetic zones that accompanied the frequent changes in sea level over the last 1 million years. This is due largely to the fact that diagenesis was controlled by numerous intrinsic and extrinsic factors that were not directly linked to sea level. The results obtained from this study parallel many of the conclusions that have been obtained from the study of young carbonate successions found on other islands in the Caribbean Sea and Pacific Ocean.

**Acknowledgements**

We are grateful to the Natural Sciences and Engineering Research Council of Canada, which funded this research (grant No. ZA635 to Jones); Henrik van Genderen from the Water Authority of the Cayman Islands who provided logistic support during the fieldwork and helped collect the samples; and Industrial Services and Equipment Ltd., Cayman Islands, who drilled wells GFN-2 and ESS-1; and Diane Caird who ran the XRD analyses. We are indebted to two anonymous reviewers and Dr. Jasper Knight (Editor) for their critical comments of the original manuscript.

**References**

Aïssaoui, D.M., Buigues, D., Purser, B.H., 1986. Model of reef diagenesis: Mururoa atoll, French Polynesia. In: Schroeder, J.H., Purser, B.H. (eds.), Reef Diagenesis. Springer-Verlag, Berlin, Heidelberg, pp. 27-52.

Beach, D.K., 1995. Controls and effects of subaerial exposure on cementation and development of secondary porosity in the subsurface of Great Bahama Bank. In: Budd, D.A., Saller, A.H., Harris, P.M. (eds.), Unconformities and Porosity in Carbonate Strata. Association of American Petroleum Geologists, Memoir 63, 1-33.

Blanchon, P., Jones, B., 1995. Marine-planation terraces on the shelf around Grand Cayman: A result of stepped Holocene sea-level rise. Journal of Coastal Research 11, 1-33.

Braithwaite, C.J.R., Camoin, G.F., 2011. Diagenesis and sea-level change: lessons from Moruroa, French Polynesia. Sedimentology 58, 259-284.

Buchbinder, L.G., Friedman, G.M., 1980. Vadose, phreatic, and marine diagenesis of Pleistocene-Holocene carbonates in a borehole; Mediterranean coast of Israel. Journal of Sedimentary Research 50, 395-407.

Budd, D.A., 1997. Cenozoic dolomites of carbonate islands: Their attributes and origin. Earth-Science Reviews 42, 1-47.

Budd, D.A., Land, L.S., 1990. Geochemical imprint of meteoric diagenesis in Holocene ooid sands, Schooner Cays, Bahamas; correlation of calcite cement geochemistry with extant groundwaters. Journal of Sedimentary Research 60, 361-378.

Budd, D.A., Vacher, H.L., 1991. Predicting the thickness of fresh-water lenses in carbonate paleo-islands. Journal of Sedimentary Research 61, 43-53.

Cant, R.V., Weech, P.S., 1986. A review of the factors affecting the development of Ghyben-Hertzberg lenses in the Bahamas. Journal of Hydrology 84, 333-343.

Clark, P.U., Dyke, A.S., Shakun, J.D., Carlson, A.E., Clark, J., Wohlfarth, B., Mitrovica, J.X., Hostetler, S.W., Mccabe, A.M., 2009. The last glacial maximum. Science 325: 710-714.

Der, A., 2012. Depositon and sea level fluctuation during Miocene times, Grand Cayman, British West Indies. Unpublished M.Sc. thesis, University of Alberta, 101 pp.

Ginsberg, R.N., Marszalek, D.S., Schneidermann, N., 1971. Ultrastructure of carbonate cements in a Holocene algal reef of Bermuda. Journal of Sedimentary Research 41, 472-482.

Gupta, B.K.S., 2003. Modern Foraminifera. Springer, Netherlands, 371 pp.

Hardie, L.A., Bosellini, A., Goldhammer, R.K., 1986. Repeated subaerial exposure of subtidal carbonate platforms, Triassic, northern Italy: Evidence for high frequency sea level oscillations on a $10^4$ year scale. Paleoceanography 1, 447-457.

Hunter, I.G., 1994. Modern and ancient coral associations of the Cayman Islands. Unpublished Ph.D. thesis, University of Alberta, 345 pp.

Jacobson, G., Hill, P.J., 1980. Hydrogeology of a raised coral atoll–Niue Island, South Pacific Ocean. BMR Journal of Australian Geology and Geophysics 5, 271-278.

James, N.P., Ginsburg, R.N., Marszalek, D.S., Choquette, P.W., 1976. Facies and fabric specificity of early subsea cements in shallow Belize (British Honduras) reefs. Journal of Sedimentary Research 46, 523-544.

Jones, B., 1992. Caymanite, a cavity-filling deposit in the Oligocene Miocene Bluff Formation of the Cayman Islands. Canadian Journal of Earth Sciences 29, 720-736.

Jones, B., Hunter, I.G., 1989. The Oligocene-Miocene Bluff Formation on Grand Cayman. Caribbean Journal of Science 25, 71-85.

Jones, B., Hunter, I.G., 1994a. Evolution of an isolated carbonate bank during Oligocene, Miocene and Pliocene times, Cayman Brac, British West Indies. Facies 30, 25-50.

Jones, B., Hunter, I.G., 1994b. Messinian (late Miocene) karst on Grand Cayman, British West Indies; an example of an erosional sequence boundary. Journal of Sedimentary Research 64, 531-541.

Jones, B., Luth, R.W., 2003. Temporal evolution of tertiary dolostones on Grand Cayman as determined by $^{87}Sr/^{86}Sr$. Journal of Sedimentary Research 73, 187-205.

Jones, B., Hunter, I., Kyser, K., 1994a. Revised Stratigraphic nomenclature for Tertiary strata of the Cayman Islands, British West Indies. Caribbean Journal of Science 30, 53-68.

Jones, B., Hunter, I., Kyser, T., 1994b. Stratigraphy of the Bluff Formation (Miocene-Pliocene) and the newly defined Brac Formation (Oligocene), Cayman Brac, British West Indies: Caribbean Journal of Science 30, 30-51.

Jones, B., Luth, R.W., Macneil, A.J., 2001. Powder X-ray diffraction analysis of homogeneous and heterogeneous sedimentary dolostones. Journal of Sedimentary Research 71, 790-799.

Land, L.S., Goreau, T.F., 1970. Submarine lithification of Jamaican reefs. Journal of Sedimentary Research 40, 457-462.

Li, R., Jones, B., 2013. Heterogeneous diagenetic patterns in the Pleistocene Ironshore Formation of Grand Cayman, British West Indies. Sedimentary Geology 294, 251-265.

Liang, T., Jones, B., 2014. Deciphering the impact of sea-level changes and tectonic movement on erosional sequence boundaries in carbonate successions: A case study from Tertiary strata on Grand Cayman and Cayman Brac, British West Indies. Sedimentary Geology 305, 17-34.

Lighty, R.G., 1985. Preservation of internal reef porosity and diagenetic sealing of submerged early Holocene barrier reef, southeast Florida shelf. In: Schneidermann, N., Harris, P.M.

(eds.) Carbonate Cements. Society of Economic Paleontologists and Mineralogists Special Publication 36, 123-151.

Lisiecki, L.E., Raymo, M.E., 2005. A Pliocene-Pleistocene stack of 57 gloabbly distributed benthic $\delta^{18}O$ records. Paleoceanography 20, 1-17.

Longman, M.W., 1980. Carbonate diagenetic textures from nearsurface diagenetic environments. American Association for Petroleum Geologists, Bulletin 64, 461-487.

Marshall, J.F., 1986. Regional distribution of submarine cements within an epicontinental reef system: central Great Barrier Reef, Australia. In: Schroeder, J.H., Purser, B.H. (eds.) Reef Diagenesis. Springer-Verlag, Berlin, Heidelberg, pp. 8-26.

Mather, J.D., 1971. A preliminary survey of the groundwater resources of the Cayman Islands with recommendations for their development. Institute of Geological Sciences, London, 91 pp.

Matley, C.A., 1926. The geology of the Cayman Islands, British West Indies, and their relations to the Bartlett Trough. Quarterly Journal of the Geological Society of London 82, 352-387.

Matthews, R.K., Frohlich, C., 1987. Forward modeling of bank-margin carbonate diagenesis. Geology 15, 673-676.

Melim, L.A., 1996. Limitations on lowstand meteoric diagenesis in the Pliocene-Pleistocene of Florida and Great Bahama Bank: Implications for eustatic sea-level models. Geology 24, 893-896.

Melim, L.A., Swart, P.K., Maliva, R.G., 1995. Meteoric-like fabrics forming in marine waters: Implications for the use of petrography to identify diagenetic environments. Geology 23, 755-758.

Melim, L.A., Westphal, H., Swart, P.K., Eberli, G.P., Munnecke, A., 2002. Questioning carbonate diagenetic paradigms: evidence from the Neogene of the Bahamas. Marine Geology 185, 27-53.

Miller, K.G., Kominz, M.A., Browning, J.V., Wright, J.D., Mountain, G.S., Katz, M.E., Sugarman, P.J., Cramer, B.S., Christie-Blick, N., Pekar, S.F., 2005. The Phanerozoic record of global sea-level change. Science 310, 1293-1298.

Naish, T.R., Wilson, G.S., 2009. Constraints on the amplitude of Mid-Pliocene (3.6-2.4 Ma) eustatic sea-level fluctuations from the New Zealand shallow-marine sediment record. Philosophical Transactions of the Royal Society 367, 169-187.

Ng, K.C., Jones, B., 1995. Hydrogeochemistry of Grand Cayman, British West Indies: implications for carbonate diagenetic studies. Journal of Hydrology 164, 193-216.

Ng, K.C., Jones, B., Beswick, R., 1992. Hydrogeology of Grand Cayman, British West Indies; a karstic dolostone aquifer. Journal of Hydrology 134, 273-295.

Peltier, W.R., Fairbanks, R.G., 2006. Global glacial ice volume and Last Glacial Maximum duration from an extended Barbados sea level record. Quaternary Science Reviews 25, 3322-3337.

Pleydell, S.M., Jones, B., Longstaffe, F.J., Baadsgaard, H., 1990. Dolomitization of the Oligocene-Miocene Bluff Formation on Grand Cayman, British West Indies. Canadian Journal of Earth Sciences 27, 1098-1110.

Quinn, T.M., 1991. Meteoric diagenesis of Plio-Pleistocene limestones at Enewetak atoll. Journal of Sedimentary Research 61, 681-703.

Quinn, T.M., Matthews, R.K., 1990. Post-Miocene diagenetic and eustatic history of Enewetak Atoll: Model and data comparison. Geology 18, 942-945.

Rohling, E.J., Foster, G.L., Grant, K.M., Marino, G., Roberts, A.P., Tamisiea, M.E., Williams, F., 2014. Sea-level and deep-sea-temperature variability over the past 5.3 million years. Nature 508, 477-482.

Schroeder, J.H., 1972. Fabrics and sequences of submarine carbonate cements in Holocene Bermuda cup reefs. Geologische Rundschau 61, 708-730.

Sherman, C.E., Fletcher, C.H., Rubin, K.H., 1999. Marine and meteoric diagenesis of Pleistocene carbonates from a nearshore submarine terrace, Oahu, Hawaii. Journal of Sedimentary Research 69, 1083-1097.

Siddall, M., Rohling, E.J., Almoogi-Labin, A., Hemleben, Ch., Meischner, D., Schmelzer, I., Smeed, D.A., 2003. Sealevel fluctuations during the last glacial cycle. Nature 423, 853-858.

Spratt, R.M., Lisiecki, L.E., 2016. A Late Pleistocene sea level stack. Climate of the Past 12, 1079-1092.

Steinen, R.P., 1974. Phreatic and vadose diagenetic modification of Pleistocene limestone: petrographic observations from subsurface of Barbados, West Indies. American Association of Petroleum Geologists, Bulletin 58, 1008-1024.

Steinen, R.P., Matthews, R.K., 1973. Phreatic vs. vadose diagenesis: stratigraphy and mineralogy of a cored borehole on Barbados, W.I. Journal of Sedimentary Research 43, 1012-1020.

Thorstenson, D.C., Mackenzie, F.T., Ristvet, B.L., 1972. Experimental vadose and phreatic cementation of skeletal carbonate sand. Journal of Sedimentary Research 42, 162-167.

Vacher, L.H.L., 1997. Introduction: varieties of carbonate islands and a historical perspective. In: Vacher, H.L., Quinn, T.M. (eds.) Geology and Hydrogeology of Carbonate Islands. Elsevier Science, pp. 1-34.

Vézina, J., Jones, B., Ford, D., 1999. Sea-level highstands over the last 500,000 years: Evidence from the Ironshore formation on Grand Cayman, British West Indies. Journal of Sedimentary Research 69, 317-327.

Vollbrecht, R., 1990. Marine and meteoric diagenesis of submarine pleistocene carbonates from the Bermuda Carbonate Platform. Carbonates and Evaporites 5, 13-96.

Vollbrecht, R., Meischner, D., 1996. Diagenesis in coastal carbonates related to Pleistocene sea level, Bermuda Platform. Journal of Sedimentary Research 66, 243-258.

Wheeler, C., Aharon, P. 1997. Chapter 17 Geology and hydrogeology of Niue. In: Vacher, H.L., Quinn, T.M. (eds.) Geology and Hydrogeology of Carbonate Islands. Elsevier Science, pp. 537-564.

Whitaker, F., Smart, P., Hague, Y., Waltham, D., Bosence, D., 1997. Coupled two-dimensional diagenetic and sedimentological modeling of carbonate platform evolution. Geology 25, 175-178.

Whitaker, F.F., Paterson, R.J., Johnston, V.E., 2006. Meteoric diagenesis during sea-level lowstands: Evidence from modern hydrochemical studies on northern Guam. Journal of Geochemical Exploration 89, 420-423.

Willson, E.A., 1998. Depositional and diagenetic features of the Middle Miocene Cayman Formation, Roger's Wreck Point, Grand Cayman, British West Indies. Unpublished M.Sc. thesis, University of Alberta, 103 pp.

Zhao, H., Jones, B., 2012. Origin of “island dolostones”: A case study from the Cayman Formation (Miocene), Cayman Brac, British West Indies. Sedimentary Geology 24, 191-206.

## Figure captions

**Fig. 1.** Geological and hydrological settings of Grand Cayman. (A) Location of Grand Cayman. (B) Geological map of Grand Cayman (modified from Jones et al., 1994a) showing distribution of Cayman Formation, location of well GFN-2, and approximate distribution of East End Lens (EEL). Distribution of EEL modified from Ng et al. (1992). (C) Schematic diagrams illustrating the present hydrological zones, and the peripheral dolostone–interior limestone distribution pattern evident from wells RWP-2, GFN-2 and ESS-1.

**Fig. 2.** Stratigraphic succession on Grand Cayman (modified from Jones et al., 1994a).

**Fig. 3.** Comparison of cored wells on Grand Cayman and sea level curve for last 1 Ma. (A) Extent of cores from the Cayman Formation in wells RWP-2, GFN-2, and ESS-1. See Figure 1B for location of wells. (B) Sea-level curve for last 1 Ma based on $\delta^{18}O$ record of benthic foraminifera from Lisiecki and Raymo (2005) and equations from Spratt and Lisiecki (2015). Note repeated highstands, highlighted by blue shading, that placed all or most of the sequences in wells RWP-2, GFN-2, and ESS-1 under water and various lowstands when all of the cored sequences in wells RWP-2, GFN-2, and ESS-1 would have been above sea level.

**Fig. 4.** Stratigraphic variations in the Cayman Formation in well GFN-2. (A) Distribution of sedimentary facies and facies associations (FA-I, II, III). (B) Distribution of diagenetic zones DZ-I, II, and III. (C) Composition of samples as determined by thin section analyses. (D) Tested porosity and permeability. (E) Distribution of calcite, LCD, and HCD as determined by XRD analyses. (F) Average %Ca of dolomite. (G) $\delta^{18}O$ and $\delta^{13}C$ of calcite and dolomite. (H) Distribution of groundwater zones as defined by chloride concentrations.

**Fig. 5.** Core photographs (A–C) and thin section photomicrographs (D–G) illustrating diagenetic features in DZ-I in well GFN-2. All depths below top well, which is 3 m asl. Thin section images in panels D and E from unstained thin section; panels F and G from thin section stained with Alizarin Red S. (A) Molds of articulated (bottom) and disarticulated (top) bivalves shells (71.2 m). (B) Molds of gastropods (73.0 m). (C) Molds of *Halimeda* plates *(H)* (57.3 m). (D) Molds of *Halimeda* plates and planktonic foraminifera (75.6 m). (E) Partial dissolution of planktonic foraminifera (83.4 m). (F) Scattered dogtooth calcite (DC) in porous limestone (90.7m). (G) Dogtooth calcite encasing and partly filling leached skeletal molds (91.7 m).

**Fig. 6.** Thin section photomicrographs showing diagenetic features in DZ-II in well GFN-2. All depths below top well, which is 3 m asl. Thin sections stained with Alizarin Red S. (A) Microcrystalline calcite cement lining walls of foraminifera and shells (14.9 m). (B) Micrite envelope encrusted by microcrystalline calcite cements (MC) (26.5 m). (C) High secondary porosity in grainstone due to dissolution of allochems. Note microcrystalline calcite (MC) encrusting the benthic foraminifera (26.5 m). (D) High porosity due to extensive dissolution of allochems. Note minor amounts of microcrystalline calcite cement (MC) around some of grains (34.4 m).

**Fig. 7.** Thin section microphotographs showing micritization (A) and dolomitization (B-D) in DZ-III in well GFN-2. All depths are from the surface of the well, which is 3 m asl. Stained with Alizarin Red S. (A) Completely micritized grains in calcitic dolostone (8.5 m). (B) Dolomite cement (DE) lining fossil mold and overlain by blocky calcite (BC) that filled the void (8.5 m). (C) Dolomite cement (arrow) around secondary pore formed by leaching of a skeletal grain or peloid (9.6 m). (D) Fabric-selective dolomitization of a skeletal allochem,

and scattered dolomite crystals. Intercrystal pores completely occluded by blocky calcite cement (9.6 m).

**Fig. 8.** Thin section microphotographs showing dissolution in dolomites (A–B) and various calcite cements in DZ-III in well GFN-2. Stained with Alizarin Red S. (A) Dolomite and hollow dolomite crystals in calcite cement (9.6 m). (B) Dolomite and hollow dolomite crystal (9.6 m) held in calcite cement. Dashed white lines indicate boundaries between large calcite crystals. (C) Two generations of calcite cements: first generation isopachous bladed cement encrusting foraminifera and second generation of drusy calcite partly filling pores (11.1 m). (D) Drusy calcite cement around grains (14.2 m).

**Fig. 9.** Stratigraphic variations in the Cayman Formation in well RWP-2. (A) Detailed sedimentary facies and one facies association (FA-IV). (B) Diagenetic zones DZ-IV, V, and VI as determined by thin section analyses. (C) Composition of samples and diagenetic zones (DZ-IV, V, VI) as determined by thin section analyses. (D) Porosity. (E) Distribution of LCD, and HCD based on XRD analyses. (F) Average %Ca of dolomite. (G) $\delta^{18}O$ and $\delta^{13}C$ of dolomite. (H) Distribution of groundwater zones based primarily on chloride concentration from EEZ-1 located on northeastern periphery of the island.

**Fig. 10.** Stratigraphic variations in the Cayman Formation in well ESS-1. (A) Sedimentary facies. (B) Distribution of LCD, HCD, and calcite (CAL) as determined by XRD analyses.

**Fig. 11.** Thin section microphotographs showing diagenetic zones in well RWP-2. All depths are from the surface of the well, which is 0.5 m asl. (A) Interparticle cavity lined with dolomite cement and then filled with two generations of caymanite (26.4 m). (B) Dolomite cement with multiple generations of dark and limpid dolomite (type G1c) (35.2 m). (C) Cavity filled with peloidal pack-grainstone and caymanite (29.9 m). (D) Dolomite cements

with multiple zones of limpid dolomite (Type G1b) (78.3 m). (E) Blocky dolomite (G2) overlying the first generation of dolomite cement (G1a) (16.6 m). (F) Two generations of internal sediments that are separated by a layer of dolomite cement (G1a, yellow arrow) (52.8 m). Note two generations of dolomite cement hanging from the roof of the cavity (green arrow).

**Fig. 12.** Oxygen and carbon isotopes of calcite and dolomite from well GFN-2 and dolomite samples from well RWP-2. Dolomite isotopes from Cayman Formation on Cayman Brac (Zhao and Jones, 2012) are shown as a comparison.

**Fig. 13.** Cumulative time of exposure of Cayman Formation at different depth over the last 1myr. Sea level data based on $\delta 18O$ record of benthic foraminifera from Lisiecki and Raymo (2005) and equations from Spratt and Lisiecki (2015).

**Fig. 14.** Correlation of the diagenetic zones of GFN-2 and RWP-2 and the present-day groundwater distribution on Grand Cayman with the last sea level transgression. Sea-level curve modified from Peltier and Fairbanks (2006).

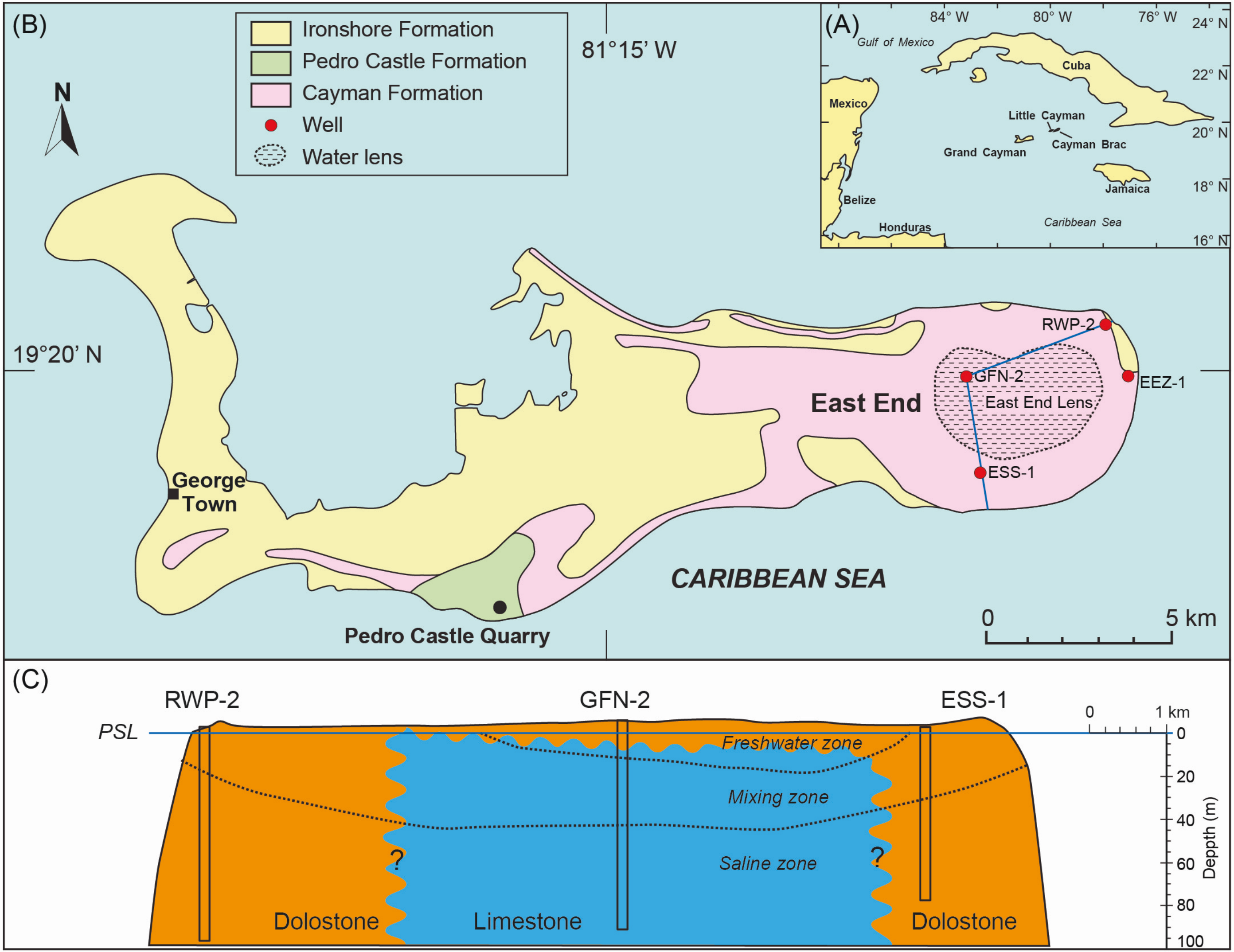

(B)
Ironshore Formation
Pedro Castle Formation
Cayman Formation
Well
Water lens
81°15' W
N
19°20' N
George Town
Pedro Castle Quarry
East End
East End Lens
RWP-2
GFN-2
EEZ-1
ESS-1
CARIBBEAN SEA
0
5 km
(A)
84° W
80° W
76° W
24° N
22° N
20° N
18° N
16° N
Gulf of Mexico
Cuba
Mexico
Little Cayman
Cayman Brac
Grand Cayman
Jamaica
Belize
Honduras
Caribbean Sea
(C)
RWP-2
GFN-2
ESS-1
PSL
Freshwater zone
Mixing zone
Saline zone
?
?
Dolostone
Limestone
Dolostone
0
1 km
0
20
40
60
80
100
Deppth (m)

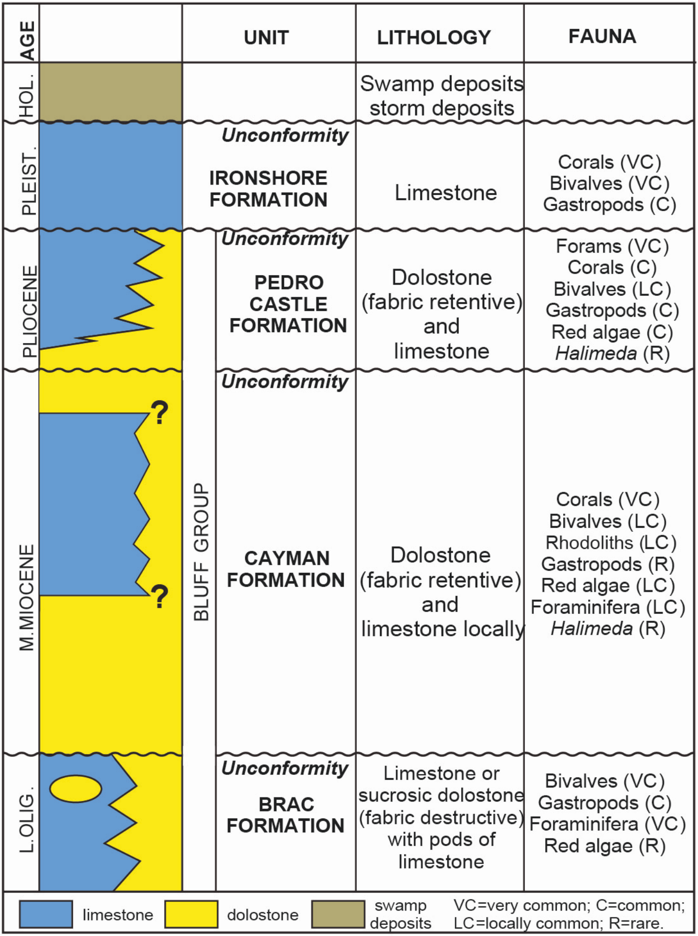
AGE
UNIT
LITHOLOGY
FAUNA
HOL.
Swamp deposits storm deposits
PLEIST.
Unconformity
IRONSHORE FORMATION
Limestone
Corals (VC)
Bivalves (VC)
Gastropods (C)
PLIOCENE
Unconformity
PEDRO CASTLE FORMATION
Dolostone (fabric retentive) and limestone
Forams (VC)
Corals (C)
Bivalves (LC)
Gastropods (C)
Red algae (C)
Halimeda (R)
M.MIOCENE
?
?
BLUFF GROUP
Unconformity
CAYMAN FORMATION
Dolostone (fabric retentive) and limestone locally
Corals (VC)
Bivalves (LC)
Rhodoliths (LC)
Gastropods (R)
Red algae (LC)
Foraminifera (LC)
Halimeda (R)
L.OLIG.
Unconformity
BRAC FORMATION
Limestone or sucrosic dolostone (fabric destructive) with pods of limestone
Bivalves (VC)
Gastropods (C)
Foraminifera (VC)
Red algae (R)
limestone
dolostone
swamp deposits
VC=very common; C=common; LC=locally common; R=rare.

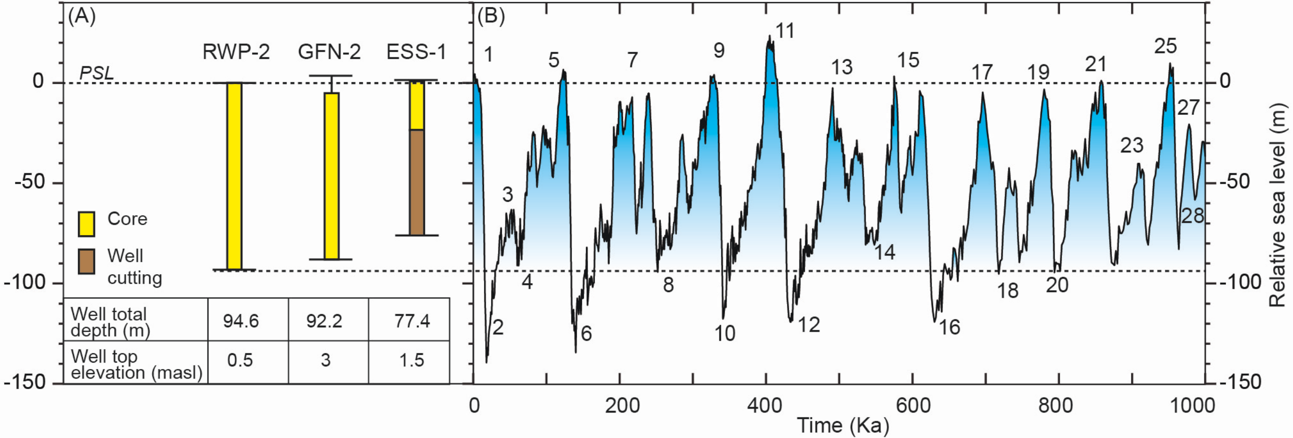
(A)
RWP-2
GFN-2
ESS-1
PSL
0
-50
-100
-150
Core
Well cutting
Well total depth (m)
94.6
92.2
77.4
Well top elevation (masl)
0.5
3
1.5
(B)
1 2 3 4 5 6 7 8 9 10 11 12 13 14 15 16 17 18 19 20 21 23 25 27 28
0
200
400
600
800
1000
Time (Ka)
Relative sea level (m)

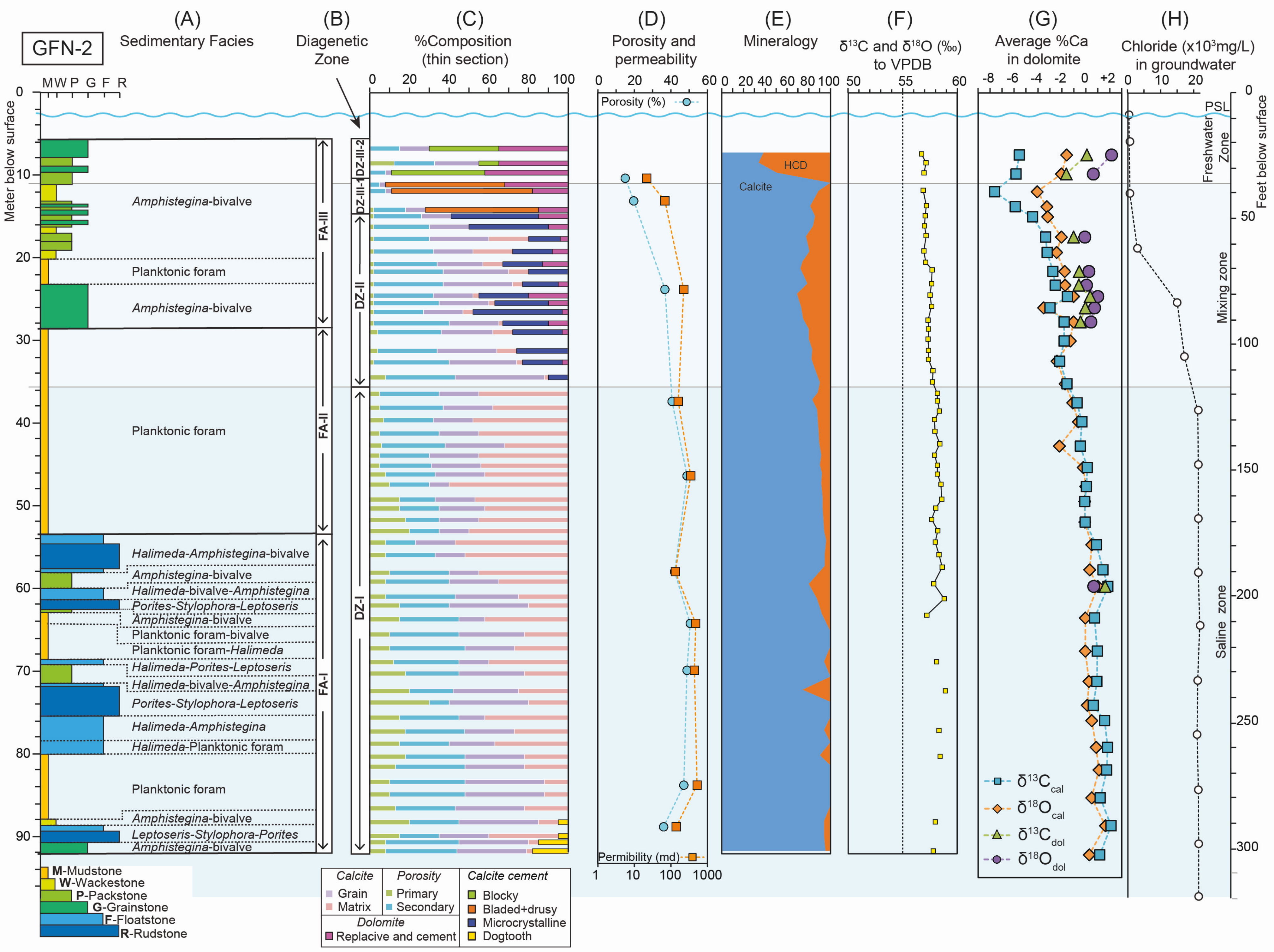
GFN-2
(A) Sedimentary Facies
(B) Diagenetic Zone
(C) %Composition (thin section)
(D) Porosity and permeability
(E) Mineralogy
(F) δ13C and δ18O (‰) to VPDB
(G) Average %Ca in dolomite
(H) Chloride (x10³mg/L) in groundwater
Meter below surface
Feet below surface
M W P G F R
PSL
Freshwater Zone
Mixing zone
Saline zone
Amphistegina-bivalve
Planktonic foram
Halimeda-Amphistegina-bivalve
Halimeda-bivalve-Amphistegina
Porites-Stylophora-Leptoseris
Planktonic foram-bivalve
Planktonic foram-Halimeda
Halimeda-Porites-Leptoseris
Halimeda-Amphistegina
Halimeda-Planktonic foram
Leptoseris-Stylophora-Porites
FA-III
FA-II
FA-I
DZ-III-2
DZ-III-1
DZ-II
DZ-I
Porosity (%)
Permibility (md)
HCD
Calcite
δ13C cal
δ18O cal
δ13C dol
δ18O dol
M-Mudstone
W-Wackestone
P-Packstone
G-Grainstone
F-Floatstone
R-Rudstone
Calcite
Grain
Matrix
Porosity
Primary
Secondary
Dolomite
Replacive and cement
Calcite cement
Blocky
Bladed+drusy
Microcrystalline
Dogtooth

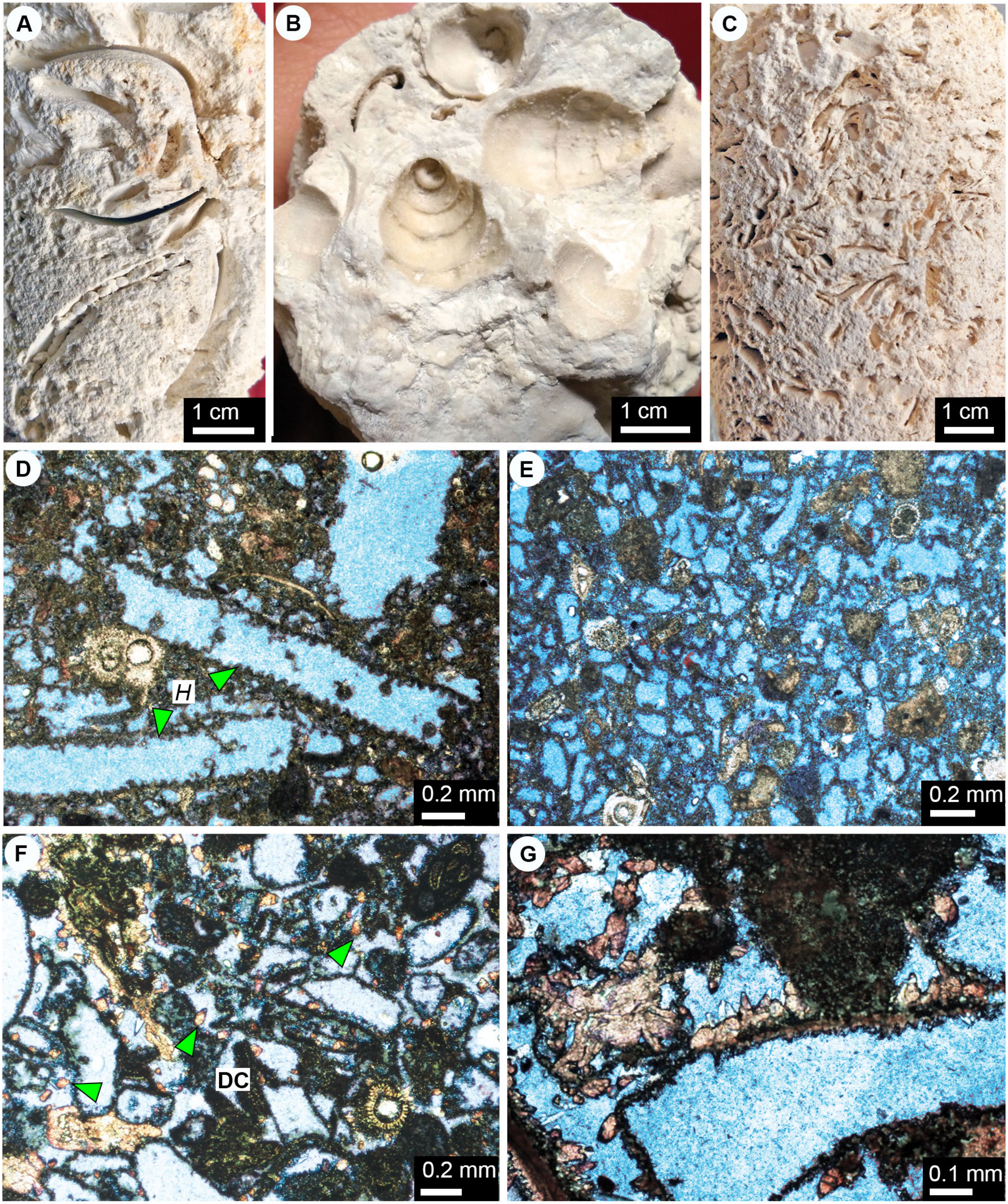
A
1 cm
B
1 cm
C
1 cm
D
H
0.2 mm
E
0.2 mm
F
DC
0.2 mm
G
0.1 mm

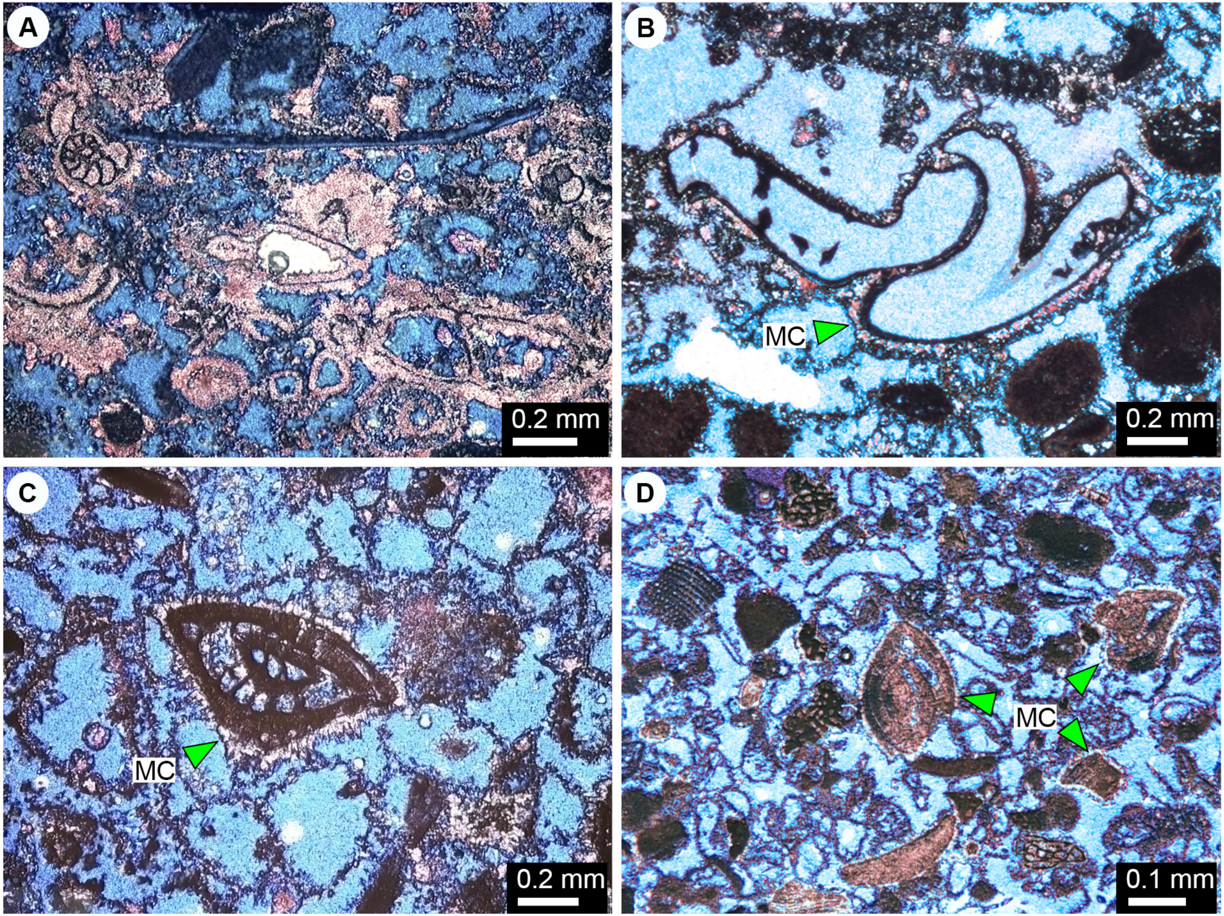
A
0.2 mm
B
MC
0.2 mm
C
MC
0.2 mm
D
MC
0.1 mm

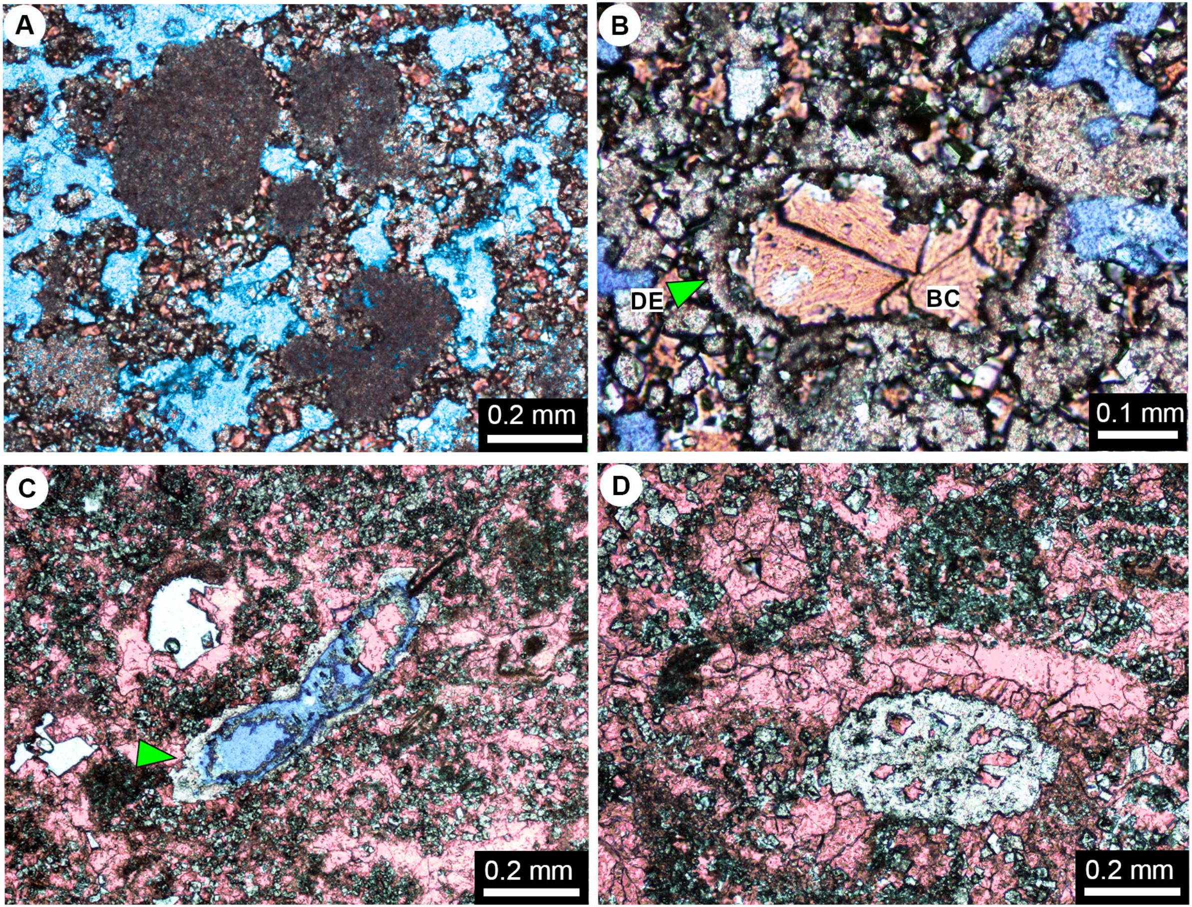
A
0.2 mm
B
DE
BC
0.1 mm
C
0.2 mm
D
0.2 mm

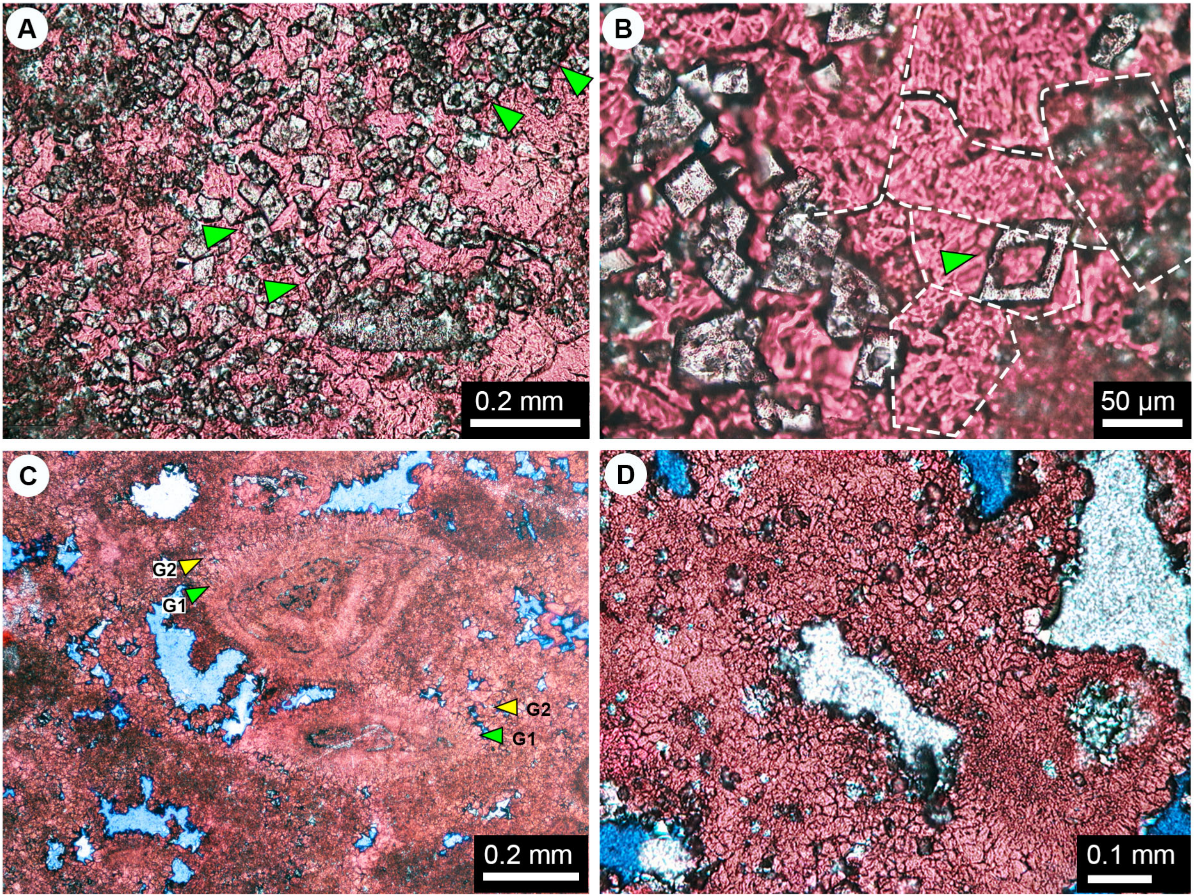
A
0.2 mm
B
50 µm
C
G2
G1
G2
G1
0.2 mm
D
0.1 mm

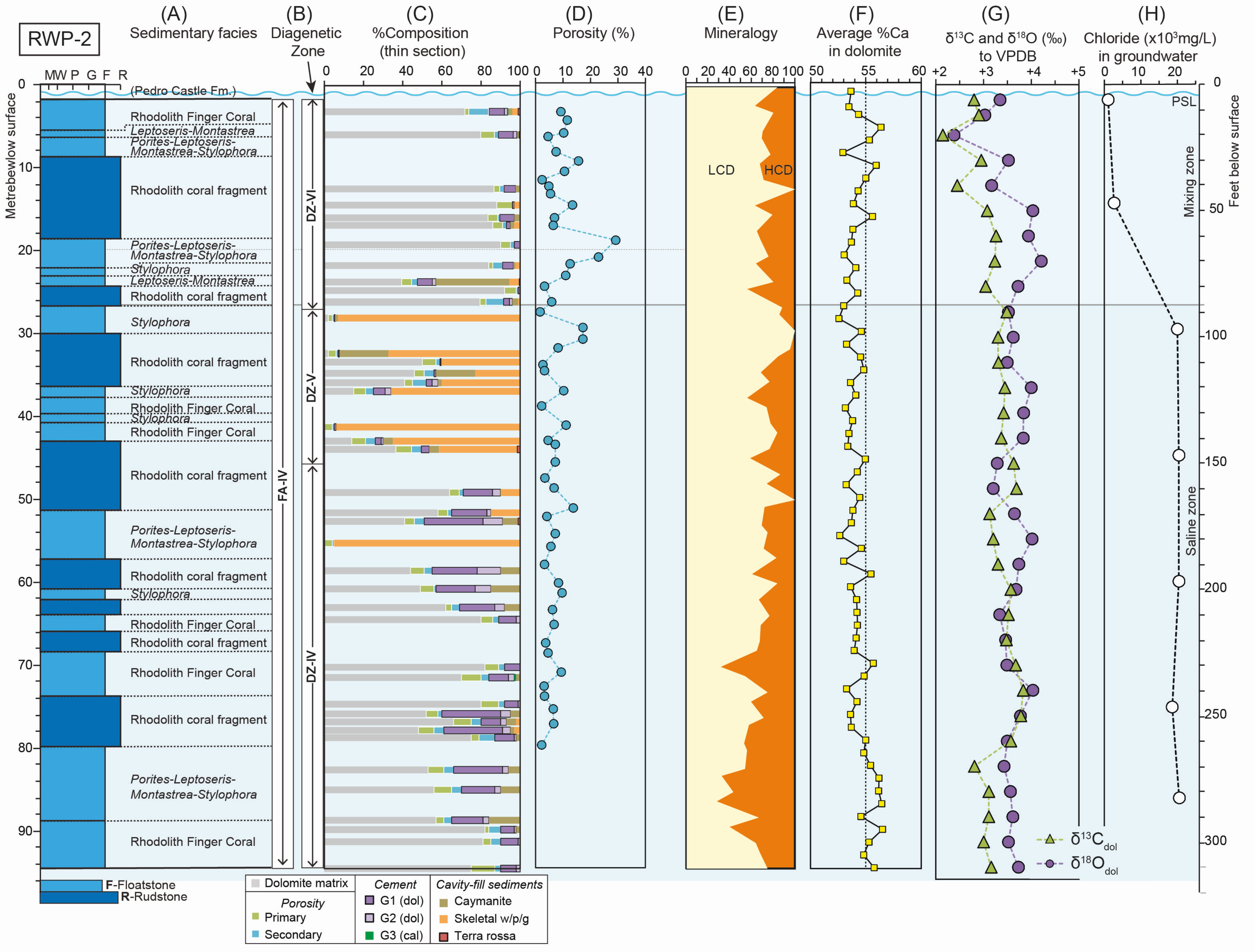

RWP-2
(A) Sedimentary facies
(B) Diagenetic Zone
(C) %Composition (thin section)
(D) Porosity (%)
(E) Mineralogy
(F) Average %Ca in dolomite
(G) δ13C and δ18O (‰) to VPDB
(H) Chloride (x10³mg/L) in groundwater
Metrebewlow surface
Feet below surface
MW P G F R
(Pedro Castle Fm.)
Rhodolith Finger Coral
Leptoseris-Montastrea
Porites-Leptoseris-Montastrea-Stylophora
Rhodolith coral fragment
Stylophora
FA-IV
DZ-VI
DZ-V
DZ-IV
LCD
HCD
PSL
Mixing zone
Saline zone
F-Floatstone
R-Rudstone
Dolomite matrix
Porosity
Primary
Secondary
Cement
G1 (dol)
G2 (dol)
G3 (cal)
Cavity-fill sediments
Caymanite
Skeletal w/p/g
Terra rossa
δ13Cdol
δ18Odol

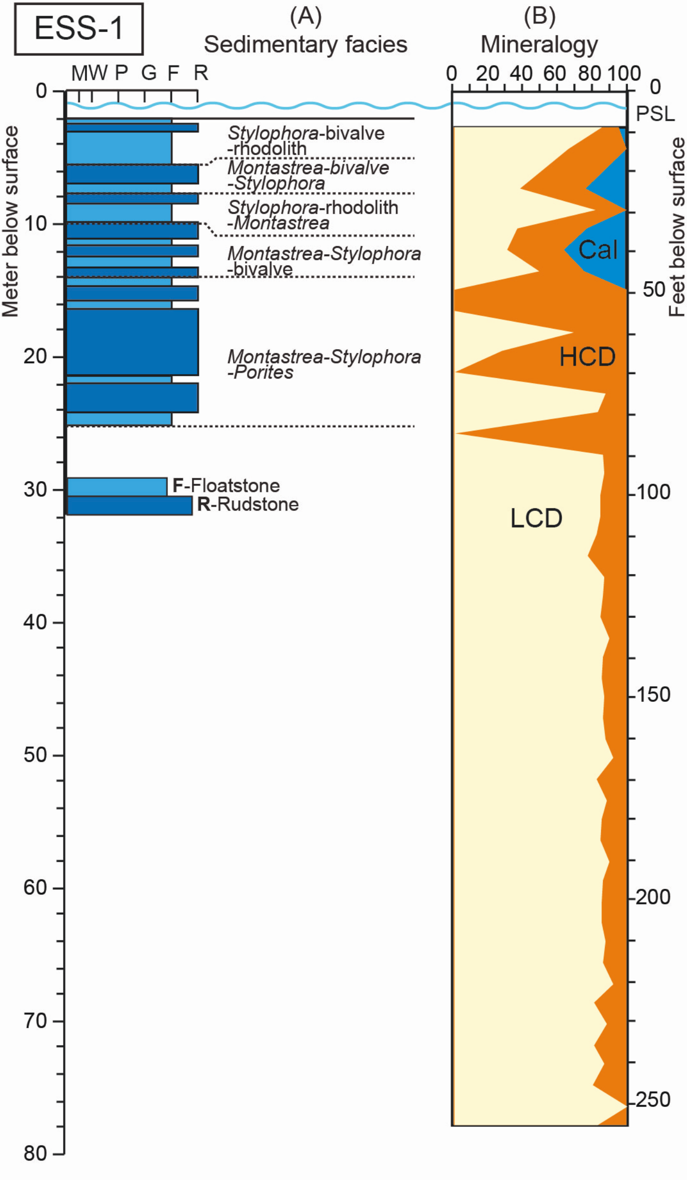

ESS-1
(A)
Sedimentary facies
(B)
Mineralogy
MW P G F R
0 20 40 60 80 100
PSL
Meter below surface
Feet below surface
Stylophora-bivalve
-rhodolith
Montastrea-bivalve
-Stylophora
Stylophora-rhodolith
-Montastrea
Montastrea-Stylophora
-bivalve
Montastrea-Stylophora
-Porites
F-Floatstone
R-Rudstone
Cal
HCD
LCD
0
10
20
30
40
50
60
70
80
0
50
100
150
200
250

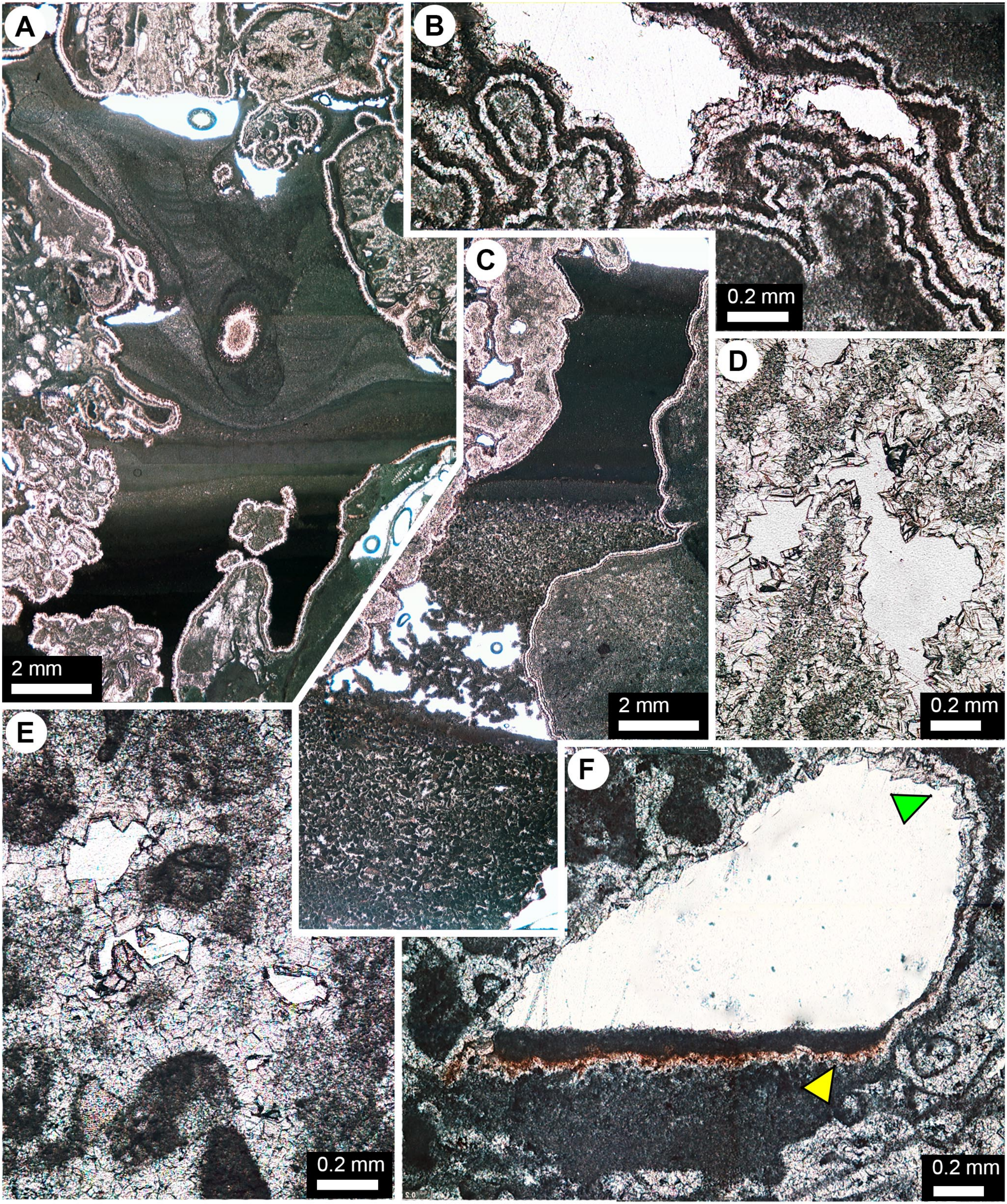
A
B
C
D
E
F
2 mm
0.2 mm
2 mm
0.2 mm
0.2 mm
0.2 mm

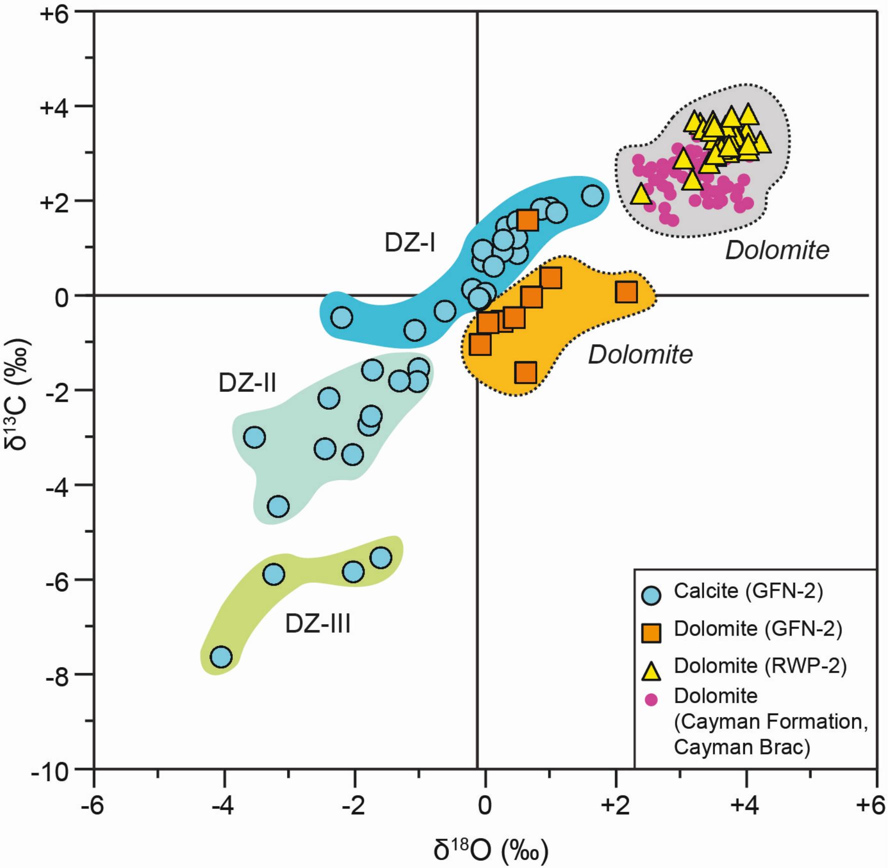

+6
+4
+2
0
-2
-4
-6
-8
-10
δ13C (‰)
-6
-4
-2
0
+2
+4
+6
δ18O (‰)
DZ-I
DZ-II
DZ-III
Dolomite
Dolomite
Calcite (GFN-2)
Dolomite (GFN-2)
Dolomite (RWP-2)
Dolomite (Cayman Formation, Cayman Brac)

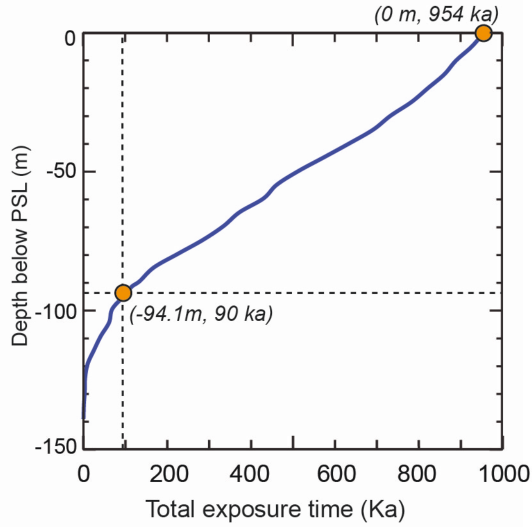

(0 m, 954 ka)
(-94.1m, 90 ka)
0
-50
-100
-150
Depth below PSL (m)
0
200
400
600
800
1000
Total exposure time (Ka)

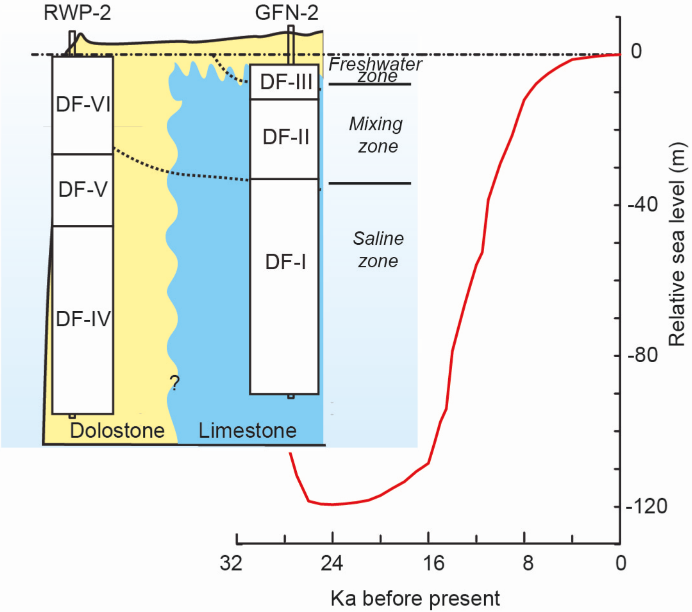

RWP-2
GFN-2
Freshwater zone
Mixing zone
Saline zone
DF-VI
DF-V
DF-IV
DF-III
DF-II
DF-I
?
Dolostone
Limestone
0
-40
-80
-120
Relative sea level (m)
32
24
16
8
0
Ka before present